Final Report

Project Title:	High Penetration of Photovoltaic Generation Study – Flagstaff Community Power
Project Period:	1/1/2011 – 1/31/2014
Submission Date:	02/27/2015
Recipient:	Arizona Public Service Company (APS)
Address:	400 N. 5th Street Phoenix, AZ 85004
Website:	http://www.aps.com
Award Number:	DE-EE0004679
Project Team:	Arizona State University (ASU) General Electric (GE) National Renewable Energy Laboratory (NREL) ViaSol Energy Solutions, LLC (VES)
Principal Investigator:	David Narang, Sr. Engineer
Phone:	602-250-4306
Email:	David.Narang@aps.com
Business Contact:	Lisa Malagon, Leader, Federal and State Compliance
Phone:	602-250-5671
Email:	Elisa.Malagon@aps.com
HQ Tech Manager:	Alvin Razon
HQ Project Officer:	Thomas Rueckert
GO Grant Specialist:	Jeannette Singsen
GO Contracting Officer:	Diana Bobo

High Penetration of Photovoltaic Generation Study – Flagstaff Community Power

Final Technical Report: Results of Phase 2-5

Period Covered: January 2011 – January 2015

February 27, 2015

Project Lead / Principal Investigator

Arizona Public Service Company / David J. Narang

Project Partners / Lead

Arizona State University / Raja Ayyanar
General Electric / Paul Gemin
National Renewable Energy Laboratory / Murali Baggu
ViaSol Energy Solutions, LLC / Devarajan Srinivasan

PREPARED FOR THE U.S. DEPARTMENT OF ENERGY SOLAR ENERGY TECHNOLOGIES PROGRAM
UNDER AWARD NO: DE-EE0004679

Disclaimer

Acknowledgements

This material is based upon work supported by the Department of Energy under Award Number DE-EE0004679. The study team gratefully acknowledges the contributions made by members of the internal and external team members, all of whom provided invaluable assistance in making this project a success. A cornerstone of this study has been the cooperation and contribution from a diverse set of groups within each organization. Their input and critique was critically important in developing the methodologies and framework described in this report. We thank them for their dedication and participation in this study.

During the course of this project, the project team included the following members:

Arizona Public Service
Erik Ellis
Hilary Waterman
Elisabeth Barras
Bryan Dellinger
Stephen Kerr
Phil Smithers
Bajarang Agrawal
Lisa Hannoush
Cyndi Newman
Gregory Teslevich
Barbara McMinn
Frank Greco
Jimi Diaz
Kevin Carroll
Tony Tewelis
Marcus Montes
Jonathan Pepper
Gerald Matli

Arizona State University
Vijay Vittal
Gerald Heydt
Yingying Tang
Qifeng Li
Titiksha Joshi
Adarsh Nagarajan
Xiaolin Mao

General Electric
Jovan Bebic
Owen Schelenz
Patrick Hart
Kathleen O’Brien

National Renewable Energy Laboratory
Tom Harris
Julieta Giraldez
Randolph Hunsberger
Bryan Palmintier
Lars Lisell

Viasol Energy Solutions
Karen Wenz

Table of Contents

List of Figures

List of Tables

Acronyms

ACC	Arizona Corporation Commission
ANSI	American National Standards Institute
API	Application Programming Interface
APS	Arizona Public Service
ASU	Arizona State University
CPP	Community Power Project (Flagstaff, AZ)
CT	Current Transformer
CYMDIST	CYME Distribution System Analysis Tool
DAS	Data Acquisition System
DG	Distributed Generation
DOE	Department of Energy
DPRES	Doney Park Renewable Energy Site
EMS	Energy Management System
EPM	Energy Profile Manager
EPRI	Electrical Power Research Institute
ESS	Energy Storage System
GE	General Electric
GHI	Global Horizontal Irradiance
GIS	Geographical Information Systems
HPSD	High Penetration Solar Deployment
HTML	Hyper Text Markup Language
Hz	Hertz
IEC	International Electro-technical Commission
IEEE	Institute of Electrical and Electronics Engineers
IT	Information Technology
kHz	Kilo Hertz
LAT	Latitude Tilt
MPPT	Maximum Power Point Tracking
MW	Mega Watt
NEC	National Electrical Code
NESC	National Electric Safety Code.
NREL	National Renewable Energy Laboratories
O&M	Operations and Maintenance
ODBC	Open Database connectivity
OLE	Object Linking and Embedding
OLEDB	Object Linking and Embedding Database
OPC	OLE for Process Control
OpenDSS	Open Distribution System Simulator
Patm	Atmospheric Pressure
POI	Point of Interconnect
PQ	Power Quality
PT	Potential Transformer
pu	Per Unit

PV	Photovoltaic
PWM	Pulse Width Modulation
QSTS	Quasi-Static Time Series
RES	Arizona’s Renewable Energy Standard
RH	Relative Humidity
rms	Root Mean Square
RTAC	Real Time Automation Controller
RTDS	Real Time Digital Simulator
SAM	Solar Advisor Model
SCADA	Supervisory Control And Data Acquisition
SCR	Short Circuit Ratio
SEL	Schweitzer Engineering Laboratories
SOAP	Simple Object Access Protocol
SQL	Structured Query Language
SV04	Sandvig Feeder 04
SV10	Sandvig Feeder 10
TCC	Time Current Curves
THD	Total Harmonic Distortion
TS	Site Temperature
UL	Underwriters Laboratories
VAr	Volt-Ampere Reactive
WAN	Wide Area Network
WS	Wind Speed

High Penetration of Photovoltaic Generation Study – Flagstaff Community Power

1. Executive Summary

APS's renewable energy portfolio, driven in part by Arizona's Renewable Energy Standard (RES) currently includes more than 1100 MW of installed capacity, equating to roughly 3000 GWh of annual production. Overall renewable production is expected to grow to 6000 GWh by 2025. It is expected that distributed photovoltaics, driven primarily by lower cost, will contribute to much of this growth and that by 2025, distributed installations will account for half of all renewable production (3000 GWh). Currently, over 850 of APS' total 1300 feeders (65%) host distributed photovoltaic generators, with over 100 feeders (8%) that have PV capacity exceeding 1 MW.

In an effort to better understand the impacts of high penetrations of photovoltaic (PV) generators on distribution systems, Arizona Public Service and its partners implemented a multi-year project to develop the tools and knowledge base needed to safely and reliably integrate high penetrations of commercial -and residential-scale PV. Building upon the APS Community Power Project–Flagstaff Pilot, this project investigated the impact of a high penetration level of PV on a representative feeder in northeast Flagstaff.

High-speed weather and electrical data acquisition systems and digital meters were installed to quantify and catalog the effects of the estimated 1.3 MW of PV that was installed on the representative Flagstaff feeder (both smaller units at homes and large, centrally located systems).

Initial objectives were to:

1. Study grid operations of a functional utility distribution feeder under an increased distributed generation condition.
2. Evaluate technical challenges of distributed PV integration with penetration levels equal to or greater than 30% of the total load.
3. Evaluate technologies and methods to ensure stable and safe feeder operation under high penetration.

One of the most important (and unexpected) conclusions that arose as the project progressed through its multiple phases was that there were no "bright line" PV-penetration standards that could be applied uniformly to all distribution feeders, such as "do not exceed a minimum-load penetration level of 50%." This occurred because as specific studies were undertaken, it was revealed that in many cases a given high penetration level on one feeder could be operationally acceptable while that same penetration level could cause material operational and safety issues on another feeder, primarily due to differences in local, feeder-specific physical characteristics. It became clear that instead of bright-line standards, what was needed were a series of flexible

and efficient modeling tools to properly equip and prepare utility system planners to evaluate, on a case-by-case basis, a nearly infinite series of combinations of feeder topologies and PV penetration levels.

Thus, as the project progressed, the initial objectives were refined to accommodate this deeper understanding of the problem and were modified to read as:

1. Study grid operations of a functional utility distribution feeder under an increased distributed generation condition.

2. Develop flexible tools that allow for the efficient evaluation of high-PV (>30%) penetration based on feeder-specific characteristics, and

3. Develop flexible tools that allow for the efficient evaluation of technologies and methods to ensure stable and safe feeder operation under high penetration on those same feeders.

These final objectives were achieved throughout the following five-phase staged approach during which the project team:

Phase 1 developed baseline models, data acquisition methods and prototypes, and performed initial evaluation of a smart inverter (Objective 1)

Phase 2 extended the baseline model to a high PV-penetration feeder. The model included coordinated operation models of connected equipment such as reclosers, capacitor banks, fuses, and PV inverters. During Phase 2, APS deployed solar PV systems and data acquisition systems under the APS Community Power Project–Flagstaff Pilot.

Comprehensive, high-resolution electrical models of the distribution system were developed to analyze the impacts of PV on distribution circuit protection systems (including coordination and anti-islanding), predict voltage regulation and phase balance issues, and develop volt/VAr control schemes (Objectives 1 and 2)

Phase 3 delivered models describing the theoretical limits of the amount of allowable PV generation on the feeder. Phase 3 also validated the developed models through extensive time series simulations and by comparison of the results with field measurements (Objectives 1 and 2)

Phase 4 extended the analysis to include grid support inverters, energy storage batteries, and more advanced topics such as: feeder reconfiguration, smart grid device interaction, intentional islanding, analysis related to harmonics content in feeder currents and voltages (Objectives 1 and 2)

Phase 5 delivered a comprehensive set of tools and processes for interconnecting PV systems including a tool for cost-benefit analysis of mitigation strategies for high-penetration. During this phase, extensive material was developed to provide documentation and training on the tools and analysis methods used during the study (Objective 3)

2. Background

DOE awarded multiple projects in high-penetration solar deployment in the last few years that are developing similar technology to the APS HPSD project as below:[1]

1. Florida State University (FSU): Sunshine State Solar Grid Initiative (SUNGRIN)[2]
2. NREL: Southern California Edison High Penetration PV
3. Sacramento Municipal Utility District: PV and Storage at Anatolia, California.
4. University of California, San Diego: Improved Modeling Tools for High Penetration.
5. Virginia State University Polytechnic Institute: Hi-Pen PV Impacts and Advanced Power Conditioning.

The APS HPSD study is distinct from the above projects, as it aims to develop practical tools and methods to help utility distribution engineers operate a distribution grid with high penetration of PV. Specifically, this study addresses feeder reconfiguration, voltage regulation, and protection coordination. During this study, the team developed multiple generic modeling tools using open source software to allow application to new feeders. The new modeling tools provide valuable analysis capability for distribution engineers and were validated against an unprecedented amount of field data.

Key project goals are to learn how to manage known challenges of high penetration distributed PV and identify areas where gaps in understanding exist. These goals allow APS to gain operational experience with high penetration PV, while contributing to collective industry knowledge.

Phase I of this study, not part of this report, developed baseline feeder models, data acquisition methodology and prototypes. Phase I also completed initial evaluation of a smart inverter.[3]

3. Introduction

APS's renewable energy portfolio, driven in part by Arizona's Renewable Energy Standard (RES) currently includes more than 1100 MW of installed capacity, equating to roughly 3000 GWh of annual production. Overall renewable production is expected to grow to 6000 GWh by 2025. It is expected that distributed photovoltaics, driven primarily by lower cost, will contribute to much of this growth and that by 2025, distributed installations will account for half of all renewable production (3000 GWh).

As solar penetration increases, additional analysis may be required for routine utility processes to ensure continued safe and reliable operation of the electric distribution network. Such processes include residential or commercial interconnection requests and load shifting during normal feeder operations. Circuits with existing high solar

[1] https://solarhighpen.energy.gov/projects/doe
[2] http://www1.eere.energy.gov/solar/pdfs/highpenforum2-02_meeker_fsu.pdf, https://solarhighpen.energy.gov/project/nrel-analysis-high-penetration-levels-photovoltaic-distribution-grid-california, http://www1.eere.energy.gov/solar/pdfs/highpenforum1-14_rawson_smud.pdf, http://www1.eere.energy.gov/solar/pdfs/sssummit2012_poster_ucsd.pdf, http://www1.eere.energy.gov/solar/pdfs/highpenforum2-03_lai_virgtech.pdf,
[3] http://www.osti.gov/scitech/servlets/purl/1025589

penetration will also have to be studied and results evaluated for adherence to utility practices or strategy.

3.1. Project Scope

Increased distributed PV penetration may offer benefits such as load offsetting, however, this also has the potential to adversely impact distribution system operation. These effects may be exacerbated by the rapid variability of PV production. Detailed effects of these phenomena in distributed PV applications continue to be studied.

Comprehensive, high-resolution electrical models of the distribution system were developed to analyze the impacts of PV on distribution circuit protection systems (including coordination and anti-islanding), predict voltage regulation and phase balance issues, and develop volt/VAr control schemes. Modeling methods were refined by validating against field measurements. To augment the field measurements, methods were developed to synthesize high resolution load and PV generation data to facilitate quasi-static time series simulations. The models were then extended to explore boundary conditions for PV hosting capability of the feeder and to simulate common utility practices such as feeder reconfiguration. The modeling and analysis methodology was implemented using open source tools and a process was developed to aid utility engineers in future interconnection requests. Methods to increase PV hosting capacity were also explored during the course of the study. A 700kVA grid-supportive inverter was deployed on the feeder and each grid support mode was demonstrated. Energy storage was explored through simulation and models were developed to calculate the optimum size and placement needed to increase PV hosting capacity. A tool was developed to aid planners in assigning relative costs and benefits to various strategies for increasing PV hosting capacity beyond current levels.

Following the completion of the project, APS intends to use the tools and methods to improve the framework of future PV integration on its system. APS further intends for the tools and methods to aid other utilities to accelerate distributed PV deployment.

3.2. Project Deployment

To support the HPSD project, APS leveraged the Community Power Project-Flagstaff Pilot by selecting the Sandvig 04 (SV04) feeder to develop, construct, and manage a high penetration of distributed PV generation.

The high penetration deployment consisted of residential, commercial, and utility scale PV systems, smart inverter technology, and data acquisition systems. APS partnered with three solar installers to pre-design the baseline PV systems, determine customer eligibility through field surveys, and install the PV systems. The eligibility criteria included grant of easement, minimum 4800 kWh annual energy consumption, and remaining rooftop age (10 y), size (enough for ≥ 2 kW), and orientation (east, south, or west) constraints. Approximately 130 residential PV systems totaling 442 kW were installed. APS installed a PV system consisting of a 333 kW ground mounted system and a 75 kW roof mounted system at an elementary school. APS installed a utility-scale 700kVA/500 kW PV system at the Doney Park Renewable Energy Site (DPRES) with the GE Brilliance® inverter and SunIQ® monitoring and control system. Feeder equipment and instrumentation are shown below in Figure 1.

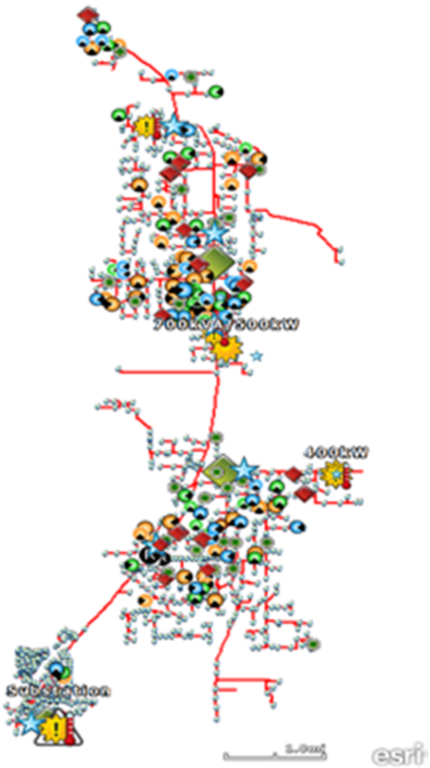

Device	Total	Legend
Substation Transformer	1	
Feeder Segments	1810	
Capacitor Banks	3	
Reclosers	2	R
Distribution Transformers	921	
Residential PV Systems	~150	
Greenfield & Commercial PV Systems	2	
Residential PV Power Quality Meter (PV DAS)	17	
Feeder Power Quality Meter (Fdr DAS)	6	
Weather Stations	4	
AMI Meters – Customer Load	~3000	Loacated at each service
AMI Meters – PV Generation	~130	Located at each PV site

Figure 1. Feeder and equipment on SV04.

Deployment Key Conclusions:

This pilot project leveraged business processes and resources in departments related to energy delivery, customer relations, distribution engineering, renewable energy, and solar O&M. Considerable effort was required in some cases to create new business processes for utility-owned assets on customer rooftops, for example new IT-related business processes and tools were developed to augment existing tools.

Careful consideration must be given to designing a data acquisition system for use in high penetration PV cases. The system must be designed to capture and synchronize both electrical and environmental data with sufficient resolution to adequately capture a variety of potentially disruptive phenomenon. Transmitting and synchronizing these data even on a small scale can provide significant storage and communication challenges. Special consideration and time must be given to ensuring that data is correctly handled as it migrates from measurement point through data concentrators to final data repository. Some redundancy may need to be built into the data acquisition deployment to mitigate unforeseen events (such as a lightning strike that destroyed one feeder data acquisition system in 2013).

4. Feeder Hosting Capacity Considerations

The feeder's load and PV generation profiles are plotted in Figure 2. As shown, SV04 is a winter-peaking feeder, with peak load occurring during the months of December and January. PV hosting capacity however is constrained not during peak load timeframe, but times of minimum daytime load, which occur during the "shoulder" months of April/May, and September/October (Min Day Load A & B). These shoulder months are also the times during which the highest PV generation and PV penetrations can be observed (Peak PV Gen, Peak PV % A & B).

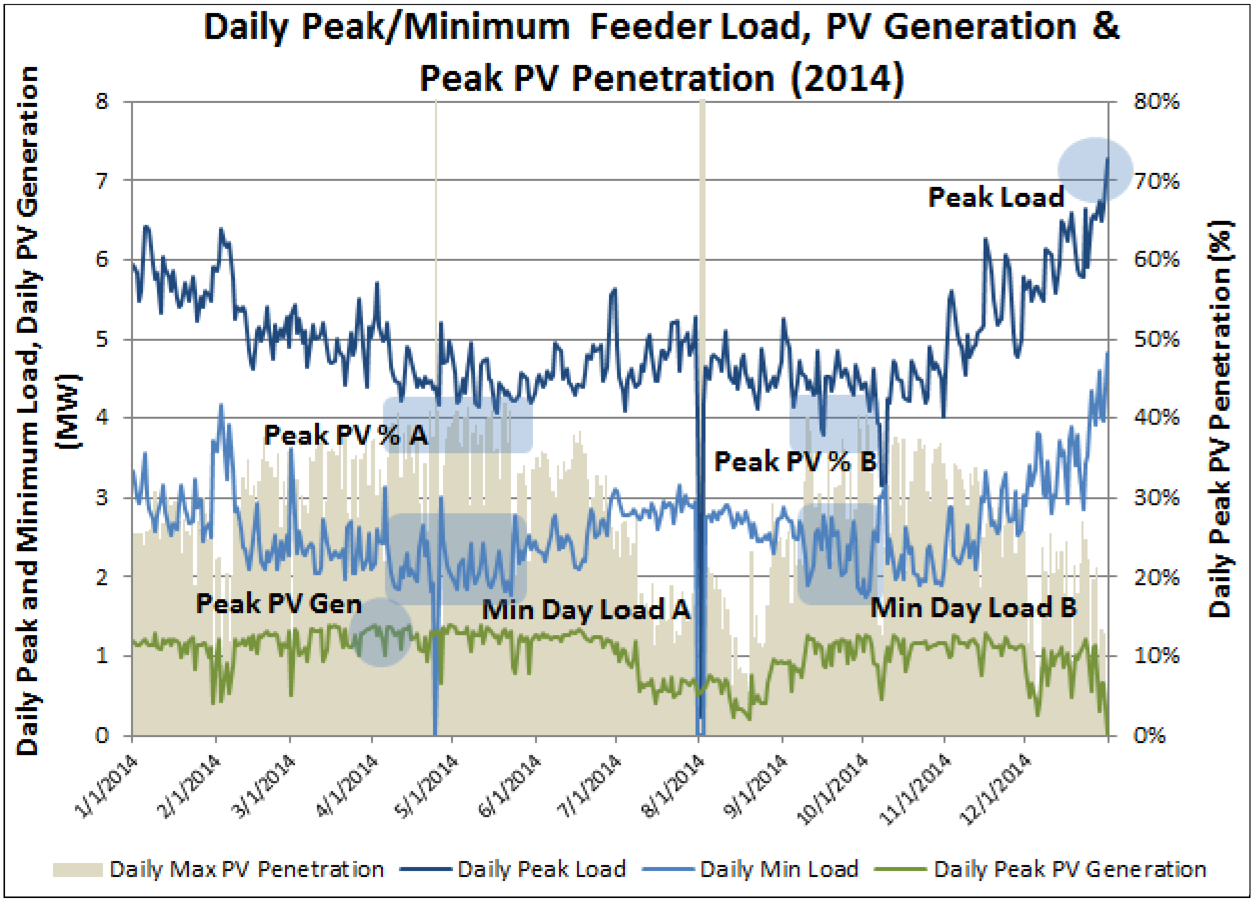

Figure 2. Feeder load and PV generation daily profile.

PV hosting capacity considerations examined during this study included safety, feeder voltage profile, and power quality. A primary safety concern was the possibility of inverter islanding. Input information for the detailed models required for this type of analysis is unavailable. Worst-case simulations performed during the course of this study showed if a large inverter fails to detect an island it can have an adverse impact on the anti-islanding schemes of smaller inverters. This however, is a highly unlikely scenario requiring perfect load and generation matching. Moreover, all inverters have some form of active anti-islanding detection.

When DG is added to the electric system, especially at high penetration levels, fault currents flowing through protective devices can increase, decrease or change directions, affecting protection coordination. Several protection issues need to be considered to analyze the impact of distributed generators on distribution systems[4][5] such as fuse-fuse coordination, fuse-recloser coordination, device sensitivity, and nuisance fuse blowing. Automated methods to verify each of these protection coordination schemes under various types and locations of faults were developed under this study.

High penetration power quality, on SV04, was examined using power quality meter measurements and harmonic power flow calculations. The harmonic spectrum was grouped into two bands: 60 Hz harmonics up to the 13th harmonic (780 Hz), and high frequency switching components above 5 kHz. High frequency equivalent circuits of various network elements were used to perform harmonic power flow studies with and without PV.

4.1. Safety

4.1.1. Inverter Anti-Islanding

Islanding is a condition where the distributed generators continue to energize a section of the distribution system after a protective device connecting the section to the main grid opens, thus forming an island of local loads and distributed generators. Islanding presents a safety hazard to personnel and may lead to equipment failure. The PV inverters are required to be tested for and comply with anti-islanding standards, for example UL 1741. A concern is whether an inverter that meets anti-islanding requirements, when tested individually in a laboratory with a simulated grid, can guarantee island detection under high penetration conditions with a large number of inverters in close proximity.

Quantifying the effects of hi-pen on inverter anti-islanding requires accurate inverter models, specifically the algorithms and parameters used in the island detection function of the inverter. These models are proprietary and generally not available. In the absence of accurate inverter models from manufacturers, typical schemes were assumed for island detection for both utility-scale three-phase inverters and single-phase residential inverters. In worst-case scenario simulations, a large inverter that fails to detect an island can have an adverse impact on the anti-islanding schemes of smaller inverters. This is a highly unlikely scenario requiring perfect load and generation matching. Moreover, all inverters have some form of active anti-islanding detection.

[4] Tony Seegers, Ken Bert, 'Impact of distributed resources on distribution relay protection', a report to the Line Protection Subcommittee of the Power System Relay Committee of The IEEE Power Engineering Society.
[5] Tarek K.Abdel, Ahmed E.B.Abu, 'Protection Coordination Planning With Distributed Generation', tech. rep., NRCan-06-0005136, Natural Resources Canada, June 2007.

4.1.2. *Protection Coordination*

Several protection issues need to be considered to analyze the impact of distributed generators on distribution systems[6,7] such as fuse-fuse coordination, fuse-recloser coordination, device sensitivity, and nuisance fuse blowing. When DG is inserted in the system, especially at high penetration levels, fault currents flowing through fuses can increase, decrease, or change directions, causing possible loss of protective device co-ordination.

The protection device coordination study was divided into two main parts – fuse-clearing scheme used by APS on SV04, and fuse saving scheme with a what-if scenario of protective device settings. The study is conducted with and without PV. Protection zones of primary-side, protective devices are shown in Figure 3. The substation relay protects the purple zone, the recloser protects the red zone, and fuses protect the blue zone. MATLAB scripts automate multiple runs of all possible fault cases to identify protection co-ordination failures.

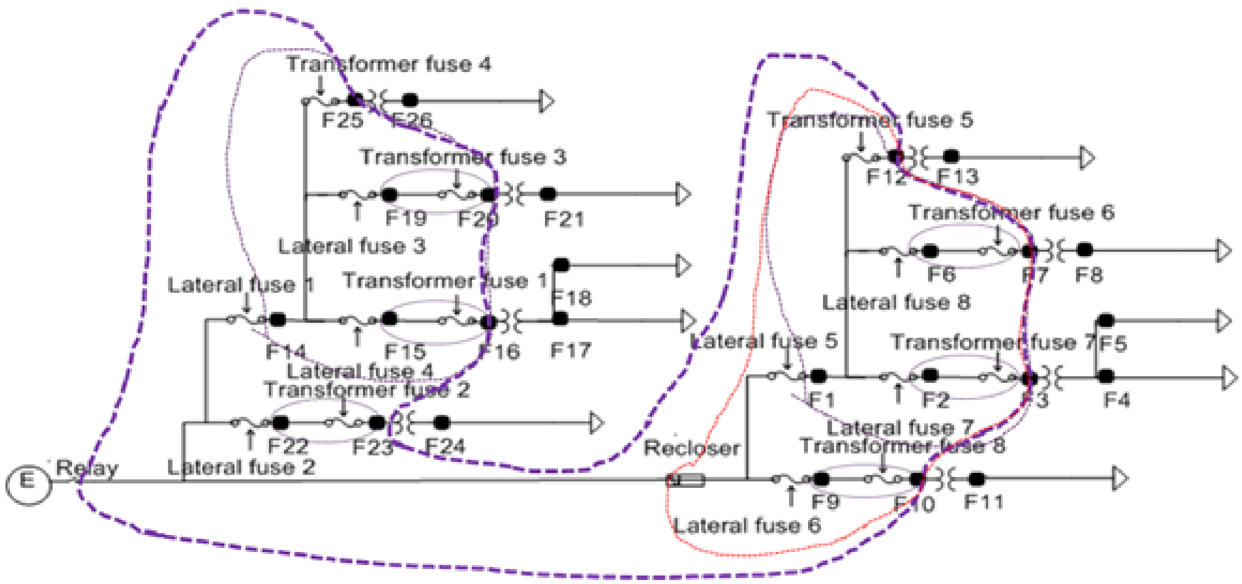

Figure 3. Fuse clearing protection zone.

Under the fuse-clearing scheme, with TCC modeled for all types of the protective devices based upon the APS settings, fuse-fuse coordination, fuse-recloser coordination, fuse-relay coordination, relay -recloser coordination were verified with and without PV systems.

Under fuse-saving scheme, the settings of the relay and recloser are changed by applying all possible fault cases without PV systems to find the proper settings that

---

[6] Tony Seegers, Ken Bert, 'Impact of distributed resources on distribution relay protection', a report to the Line Protection Subcommittee of the Power System Relay Committee of The IEEE Power Engineering Society.

[7] Tarek K.Abdel, Ahmed E.B.Abu, 'Protection Coordination Planning With Distributed Generation', tech. rep., NRCan-06-0005136, Natural Resources Canada, June 2007.

achieve all the coordination types. Then all the coordination types are studied and verified with the new protective device settings when PV is included in the feeder with varying outputs. Under this scheme, PV fault current contribution does not cause loss of coordination.

Protection coordination was also studied on another feeder (SV10) under the fuse-clearing scheme. SV10 contains 3 reclosers, 97 lateral fuses, and 26 residential PV systems. Since residential PV systems do not affect coordination, these systems are ignored. A total of 342 cases were studied for the lateral fuse-lateral fuse coordination. In this scenario, coordination failure occurs in 24 of the 342 cases. In these cases, loss of coordination occurs between upstream K65 fuse and downstream T40 fuse combinations. The upstream fuse K65 operates faster than the downstream fuse T40 when fault current exceeds 300 A. This suggests a need for revising fuse sizes.

The other types of coordination studied under this scheme, lateral fuse-relay (15 cases), lateral fuse-recloser coordination in the area downstream of each of the three reclosers, recloser to relay coordination (573 cases), showed no loss of coordination.

Protection Coordination Key Conclusions

Protection coordination study is time-consuming exercise requiring detailed and accurate information for all related devices such as substation relay, reclosers, transformer fuses, lateral fuses, any fuses in switching cabinets, and PV inverters. GIS data should be scrutinized and verified with distribution engineers to ensure that all devices have been correctly identified and modeled. Many combinations of faults need to be studied under various strategies such as fuse-clearing or fuse-saving. A way to automate multiple runs of all possible fault cases will be required (the team used MATLAB for this automation).

4.2. Power Quality

4.2.1. Harmonics

High penetration power quality, on SV04, was examined using power quality meter measurements and harmonic power flow calculations. The harmonic spectrum was grouped into two bands: 60 Hz harmonics up to the 13^{th} harmonic (780 Hz), and high frequency switching components above 5 kHz. High frequency equivalent circuits of various network elements were used to perform harmonic power flow studies with and without PV[8].

Night time measurements and simulations were used to determine harmonic content on the feeder without PV. In mid-July 2013, measured temporal variation at one DAS location showed voltage THD exceeding 9% around 7:00 PM. Odd harmonics, starting at the third harmonic, dominated the current spectrum. For simulation, the base current magnitude was set using AMI meter data. The current spectra was set equivalent to

[8] T. Joshi, G. Heydt, R. Ayyanar, "High frequency spectral components in distribution voltages and currents due to photovoltaic resources," North American Power Symposium (NAPS), 2014, pp. 1-6.

non-linear rectifier loads. Simulated spatial variation along the feeder showed voltage THD increasing from feeder head to feeder end. Table 1 shows the measured versus simulated voltage THD values on SV04 at night time. The feeder DAS measured current spectra, which can be used for simulations to improve the results.

Table 1. Measured vs Simulated Voltage THD

Location	Va Meas	Va Sim	Vb Meas	Vb Sim	Vc Meas	Vc Sim
RM26	5.66	6.32	6.03	6.17	6.15	5.72
RM23	5.76	6.20	5.73	5.93	5.69	5.62
RM27	5.42	5.65	5.35	5.41	5.14	5.16
RM25	4.07	3.30	3.90	3.13	4.22	3.02
RM1	0.38	0.45	0.42	0.43	0.38	0.42

Current THD values from inverter datasheets were used to set current harmonic spectra of all PV inverters along the feeder with real power set to 85% of the rating. Harmonic power flow study was conducted with customer load set to a typical noon in September. Maximum voltage distortion in any phase was calculated to be 3.0%. The generation at the 400kW elementary school PV site (commercial PV site) results in a current distortion of 3.0%, along with high voltage distortion, as several, close-proximity PV systems inject high frequency currents into this bus.

The driving point impedances and transfer impedances at critical points along the feeder can be important in analyzing the power quality effects of high penetration PV. These impedances are obtained in OpenDSS by injecting one ampere current into a specific bus of interest at various frequencies other than the fundamental, and calculating the resulting voltage responses. The voltage response at the same bus is equal to its driving point impedance. The voltage response at a close-proximity bus is the transfer impedance between the two buses. Impedance plots will reveal resonance conditions in the feeder, if any. In this study, low (< 40th harmonic) frequency and high frequency (2–20 kHz) scan analysis are performed. The commercial PV site is selected as the bus of interest. Its driving point impedance and transfer impedance to the capacitor bank close to that lateral are examined. AMI data is used for loads.

At low frequencies, two peaks are observed on the transfer impedance between the commercial PV site bus and the near-by capacitor banks - at 350 Hz and 936 Hz. The impedance (Za, Zb, Zc) magnitude and voltage distortion at these peaks is given in Table 2.

Table 2. Impedance and Distortion for Low Frequency Scan

Frequency	Za Ohms	Va Distortion	Zb Ohms	Vb Distortion	Zc Ohms	Vc Distortion
350 Hz	2.53	3.4%	2.04	2.7%	2.47	3.3%
936 Hz	4.88	6.6%	3.71	4.9%	4.18	5.6%

The high frequency scan ranges from 2 kHz up to 20 kHz. For the high frequency scan, the OpenDSS model was improved to include high frequency effects like the π distributed model of long lines, skin effect at high frequencies, and transformer inter-winding capacitances. By assessing the driving point impedance plots, for positive and zero sequences, at various frequencies, the following are then determined:

1. Parallel resonant conditions as peaks of impedance magnitude
2. Series resonant conditions as minima in impedance magnitude
3. Potential high values of positive, negative, or zero sequence voltage components at a bus

Positive-sequence, parallel resonance, at Doney Park, occurs at 5.90 kHz, 5.91 kHz, and 7.47 kHz for the three phases. Series resonance occurs at 11.2 kHz. For the zero sequence components, parallel resonance occurs at three frequencies for each phase. Switching off the capacitor bank moves the resonant frequencies to higher frequencies.

To determine bus voltage distortion, harmonic currents determined by the inverter power and current THD ratings are injected at different PV locations: residential, commercial PV site, and DPRES. The bus voltage distortion was calculated for the highest penetration case as determined from measured data. Voltage distortion was highest at PV connected buses and at the end of single phase laterals where the system is weak.

The carrier frequencies of inverters from different manufacturers vary from each other. Inverters from the same manufacturer, which may have the same frequency, are still typically asynchronous. Simulations are performed for the worst-case condition of synchronous carrier frequencies, and for a representative, random phase difference between the carrier frequencies. The maximum bus voltage distortions corresponding to these two conditions at two different frequencies are shown in Table 3.

Table 3. Voltage Distortion for Synchronous and Random Phase Sequence

Frequency (kHz)	Injection current phase assumption*	Maximum individual voltage distortion		
		phase A	phase B	phase C
12	Synchronous	3.03%	3.50%	2.17%
12	Random	2.18%	2.19%	2.16%
16	Synchronous	3.19%	3.03%	3.24%
16	Random	2.58%	2.65%	2.63%

4.2.2. Flicker

Voltage flicker is low frequency modulation of the 60 Hz nominal voltage waveform. Typical values of frequency components for flicker studies are generally less than 10 Hz and often less than 8 Hz. These components are in the region in which the human eye is sensitive, and it is known that most people can recognize fluorescent lamp flicker down to about 0.5% bus voltage variation at 7 Hz flicker frequency.

GE developed a digital flicker meter based on IEC 61000-4-15, which establishes standards to quantify flicker level. The tool was developed in MATLAB and was used to analyze voltage fluctuations due to PV variability. The key components of the tool include cyclic rms voltage normalization, lamp-eye-brain chain response, and statistical assessment. The tool was calibrated using input voltage waveforms in IEC 61000-4-15 to within ±5% relative error. Sampling frequency, number of bins, input voltage normalization, and computation methods affect the accuracy of the tool. The tool can deal with a single time series, or multiple series for comparison and correlation studies. The observation duration and moving step size can be adjusted. Windows can be selected to limit data.

The tool was used to determine voltage flicker under different inverter operating modes at DPRES for a clear and cloudy day.

Main observations from analysis include:

1. In all cases, the short-term flicker metric was relatively low, within the IEC power quality limit of Pst = 1.0, and dominated by load variations.
2. Voltage regulation activities caused spikes in the flicker metric.
3. PV generation variability had a negligible effect.
4. The active voltage regulation mode maintained the line voltage minimizing flicker, but measurement noise and control loop dynamics could induce additional flicker under varying circumstances.

4.3. Reliability

Annual reliability indices for the feeder during a period of six years are shown in Table 4. The time frame captures reliability indices in relation to PV capacity ranging from a period of low PV capacity on the feeder in 2009 (roughly 40 kW) to a high penetration level in 2012-2014 of roughly 1.5 MW. Deployment of all PV installations was completed by 4/9/2012. Additional feeder data must be analyzed to determine if any trends exist but the information is presented here as a baseline.

Table 4. Reliability Indices for SV04

Reliability Index	2009	2010	2011	2012	2013	2014
SAIFI	3.70	0.64	1.45	0.13	1.34	2.65
SAIDI $_{hr.}$	19.83	1.48	2.15	0.21	2.59	4.14
CAIDI $_{hr.}$	5.36	2.33	1.49	1.65	1.93	1.56
MAIFI	1.73	0.86	0.06	3.43	1.48	1.02
Sustained Outage Root Cause						
Foreign Interference	2	4	1	-	3	4
Scheduled	2	-	5	-	8	14
Substation Related	2	-	-	-	-	-
Underground Cable	4	5	7	8	5	9
Other/fuse or OCR operation	1	-	1	4	1	2
Equipment Failure	-	1	2	1	8	3
Weather, Storm/Fire, Lightning - related	5	9	10	4	5	7
Totals						
PV Capacity (MW AC)	0.04	0.12	0.48	1.44	1.44	1.44
Sustained Outages	16	19	26	17	30	39
Momentary Outages	7	3	6	7	4	4
Customer Base	3165	3188	3076	2949	3107	3159

SAFI[9] (System Average Interruption Frequency Index) is a measure of the frequency of sustained outages experienced by the average customer. 2009 and 2014 SAIFI are high relative to the other years; however it can be seen that 2012 was one of the lowest years during the six years shown and that 2013 (higher PV) was lower than 2011.

SAIDI $_{hr.}$ (System Average Interruption Duration Index) in 2009 showed an average of 19.83 hours of interruption for the average customer during the year. The trend does seem to go up in 2013 and 2014 relative to 2010 and 2011 (4.14 hours) but again, 2012 shows one of the lowest duration of interruption during the six years.

[9] IEEE Guide for Electric Power Distribution Reliability Indices, IEEE Standard 1366-2012, 2012

CAIDI $_{hr.}$ (Customer Average Interruption Duration Index) indicates the average time to restore service and seems to be generally trending downward since a high of 5.36 hours in 2009. The 2014 number of 1.56 hours is the second lowest recorded in the six years shown.

MAIFI (Momentary Average Interruption Event Frequency Index) is indicative of the average frequency of momentary events (events lasting less than or equal to 5 minutes). The MAIFI index for 2014 is 1.02, which is the 3rd lowest in the six years shown (2009 is the highest in the six years (1.73)).

Records indicate that total sustained outages in 2013 and 2014 seem to be trending up relative to the previous four years: 30 outages in 2013, 39 in 2014, up from 16 outages in 2009 however this could be caused by scheduled and/or storm-related outages.

Based on the overall data recorded to date however, it is unclear if high penetration solar affects reliability on this feeder.

4.3.1. Voltage Regulation

High penetration PV affects voltage regulation along the feeder impacting capacitor bank operation. Capacitor bank operation is automated without feedback (instrumentation). Hence, an analytical method is used to determine capacitor bank switching. Voltage (dV/dt) and reactive power (dQ/dt) ramps are calculated from feeder DAS data. Any ramp less than half the capacitor bank rating (300 kVA) were removed. The remaining ramp events are tied to capacitor bank switch on (negative ramp) and switch off (positive ramp). Two switching event-pairs per day occur Monday through Wednesday, one pair Thursday through Saturday, and no switching events on Sunday for a total of nine switching events per week.

A volt-VAR study was conducted using QSTS simulations to verify interaction of capacitor banks with PV. PV does not alter circuit behavior due to high stiffness ratio and conductor configuration.

4.3.2. Voltage Sensitivity Analysis

Voltage sensitivity to reactive power events were analyzed by comparing voltage ramps to reactive power ramps. Ramp events with changes greater than 1% are classified as major ramp events. All DAS locations were analyzed and the substation analysis was presented, as an example in Figure 4. Some of the voltage changes exhibited a negative correlation with reactive power changes due to capacitor bank switching – some voltages increase even though reactive power decreases. The histograms show most voltage ramp events are within 0.5% of nominal, and all ramps were within 2%. These sensitivities will vary spatially along the feeder. The major ramp events in Figure 4, greater than 50% of cap bank size (0.3 MVA), correspond to cap bank switching.

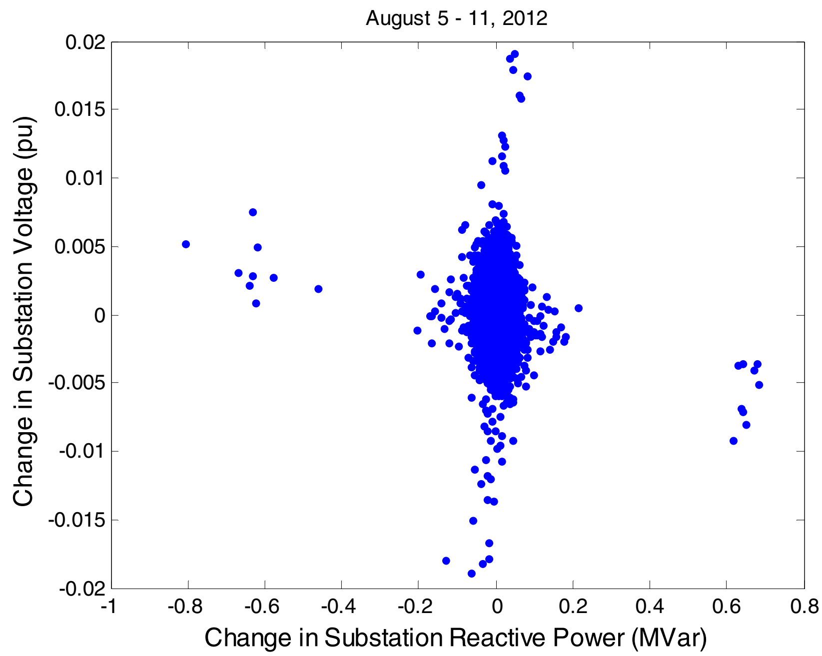

Figure 4. Voltage variation with reactive power at substation.

In addition to the feeder DAS data, operational data from the SunIQ system at DPRES was used to determine voltage sensitivity to reactive power during active and reactive power modes of the inverter. One-second SunIQ data was averaged over 1-minute. Reactive-power-mode, voltage sensitivity at DPRES is shown in Figure 5.

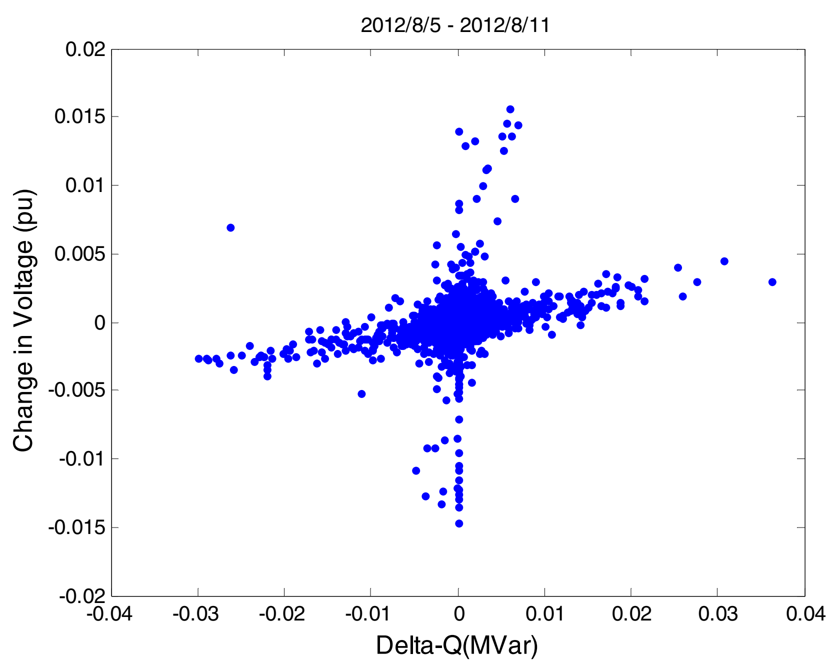

Figure 5. Reactive-power-mode, voltage variation at DPRES.

Voltage Regulation Key Conclusions

Capacitor banks were not instrumented to record switching events; therefore an analytic method was developed to determine capacitor-bank-switching based ramps in voltage and reactive power. Quantitative methods were used to determine sensitivity of voltage variations to major grid events such as capacitor bank switching, active power ramp and reactive power changes in solar power plants. These algorithms were implemented in Matlab and used to analyze the field data from the feeder DAS and inverter data. These methods proved effective to determine capacitor bank switching and to determine voltage sensitivity to grid and inverter events. There is a decrease in voltage ramp rate with distance from the feeder head. There is also a strong correlation of POI voltage at DPRES with active and reactive power output from the inverter but overall, PV does not alter circuit behavior due to high stiffness ratio and conductor configuration.

4.4. Interconnection and Analysis

NREL developed a recommendation for future interconnection assessment methodology as shown in the block diagram of Figure 6. This methodology was tested for SV04 and SV10. The methodology was based on QSTS simulations, and the implementation of interconnection scenarios and analysis of potential mitigation strategies.

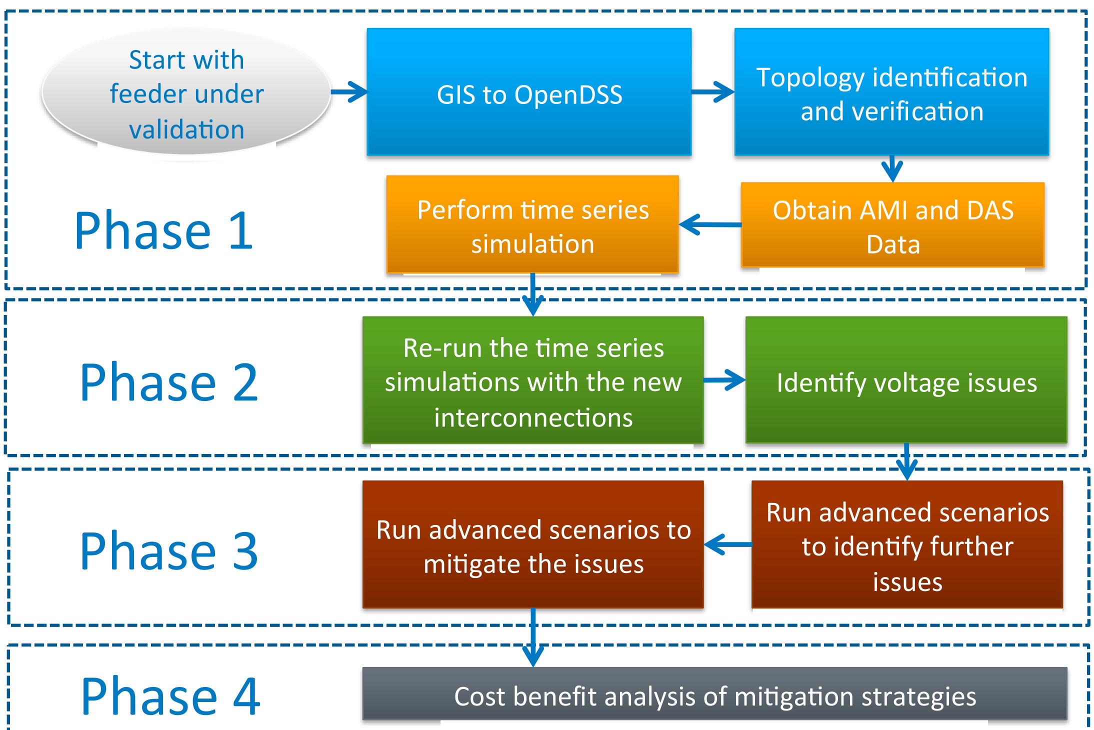

Figure 6. Interconnection assessment methodology flowchart.

The advanced scenario analysis options are shown in Figure 7. Base case scenarios for a given feeder, for a user-defined time period are evaluated initially and the results are analyzed using the visualization tools. Next, an interconnection analysis scenario for a new PV system on one of the feeders was evaluated. The inputs include the location and size of the PV system. The results of the interconnection scenario analysis are examined using the visualization tools to check for any voltage violations in the system. If voltage violations exist, four different mitigation strategies can be evaluated by the user, as follows:

1. Adjustment of capacitor bank settings (modify capacitor settings or disable)
2. Advanced inverter operation 1 (modify power factor setting of a PV inverter)
3. Advanced inverter operation 2 (enable volt-var control of a PV inverter using a user specified curve)
4. Advanced inverter operation 3 (enable dynamic control of a PV inverter using user specified bandwidth and delay settings)

In addition, the user can check for feeder reconfiguration scenarios for two feeders, for the base case or with the newly added PV systems to determine voltage violations. In this example, reconfiguration location options include:

1. Near the substation
2. Midway
3. Far from the substation

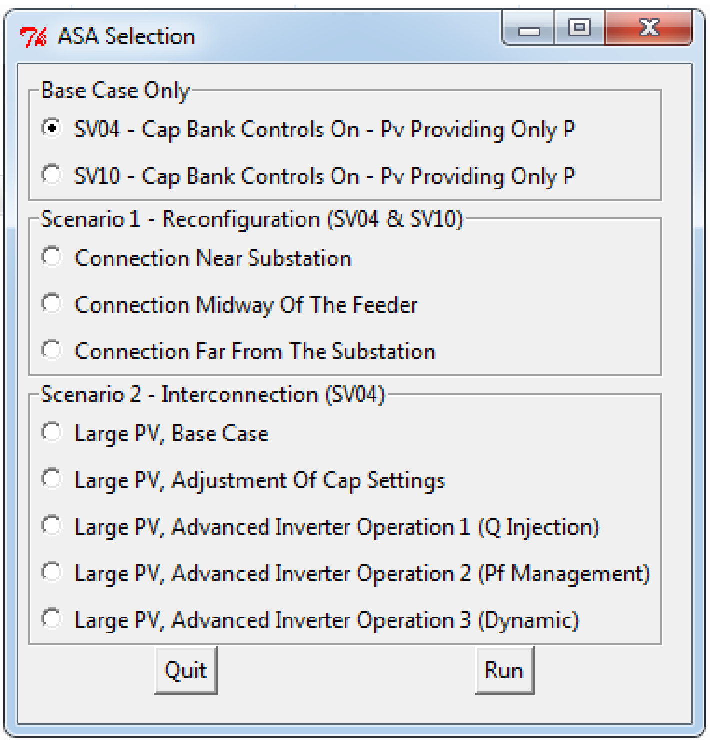

Figure 7. Advanced scenario analysis tool.

Interconnection and Analysis Key Conclusions:

The PV interconnection and analysis methodology developed here is intended to provide a framework and open-source toolkit for creating a yearly steady-state simulation to determine voltage issues resulting from PV. If voltage events are detected through the analysis, various mitigation schemes can be developed and studied using the tool. The process is an improvement over existing methods that do not account for existing PV on the feeder. Actual field data from AMI meters is used to exercise the models rather than assumed loading levels, which should improve the accuracy of results. As practitioners gain fluency with the tool it is expected they will find ways to create additional functionality. When applying the methods to other feeders, additional effort will be required to compile and format the various input files needed for the analysis. New business or IT process will need to be created to ensure the data exchange can be made in a smooth and timely manner. Additional training will also be required to familiarize engineering staff with the tools and methods.

4.5. Visualization Toolkit

Improved visualization of field data and model results can be used to inform O&M and system planning personnel of PV hosting capacity. Hence, the project team developed several tools and incorporated them into the APS platform.

APS implemented a data collection and archival platform in Phase I. To further support the project, APS added a new database server, application server, and other web servers. The improved system architecture is shown in Figure 8. The data processor system was upgraded from a Desktop Windows Application to a Windows Service on the APS Application Server. The data retrieval process from PI was changed from ODBC to OLEDB resulting in 4x improvement in retrieval speeds. The SQL server stores PI data and other datasets, and it is a data hub for data processing and visualization applications. Data is retrieved from the SQL server using a web-based HTML form tool. The tool is set up to include data from a variety of sources. The data from different sources are time-aligned, collated, error-checked, and formatted into one output file.

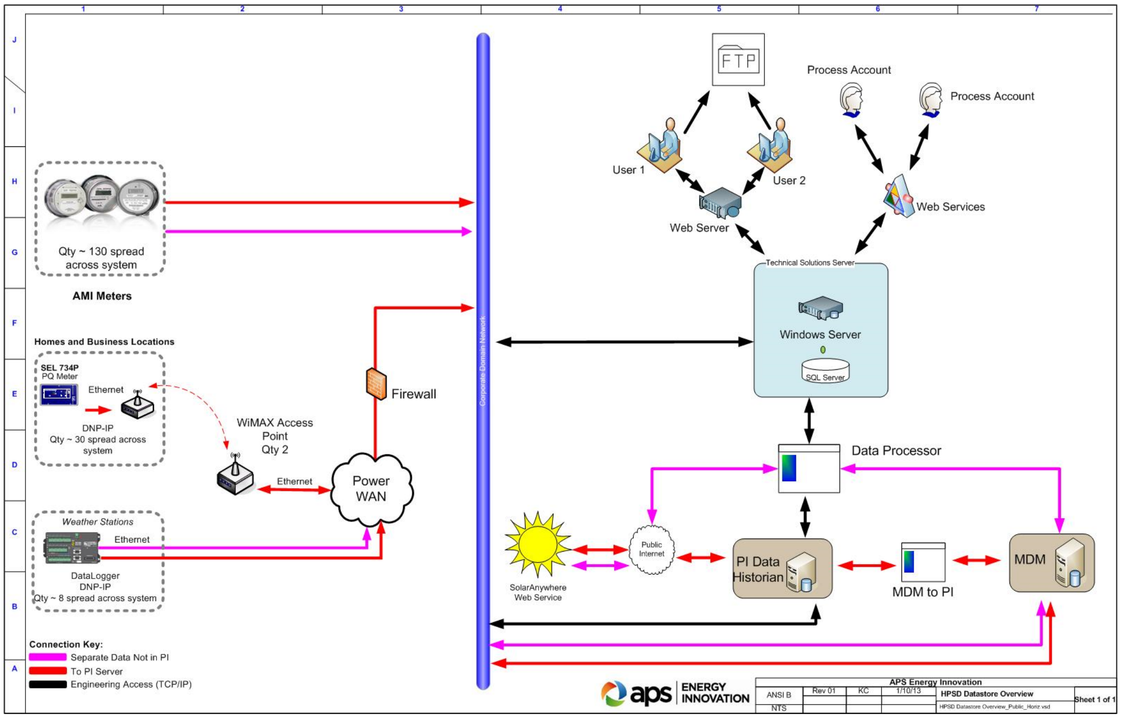

Figure 8. Improved visualization platform data architecture.

4.5.1. SAM Application Programming Interface

NREL Solar Advisor Model (SAM) was integrated into the APS visualization platform using an application programming interface (API). NREL created the C# API, which can be called iteratively within the APS visualization platform. APS used a SOAP (Simple Object Access Protocol) web service to integrate the SAM API as shown in Figure 9. The API is used with a variety of input irradiance sources to estimate PV production. This estimate is then compared with actual PV production to improve the estimation model as shown in Figure 10.

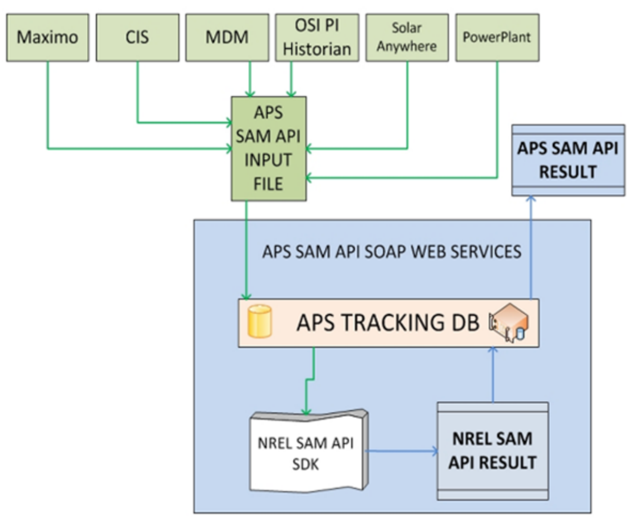

Figure 9. SAM API integration into APS visualization platform.

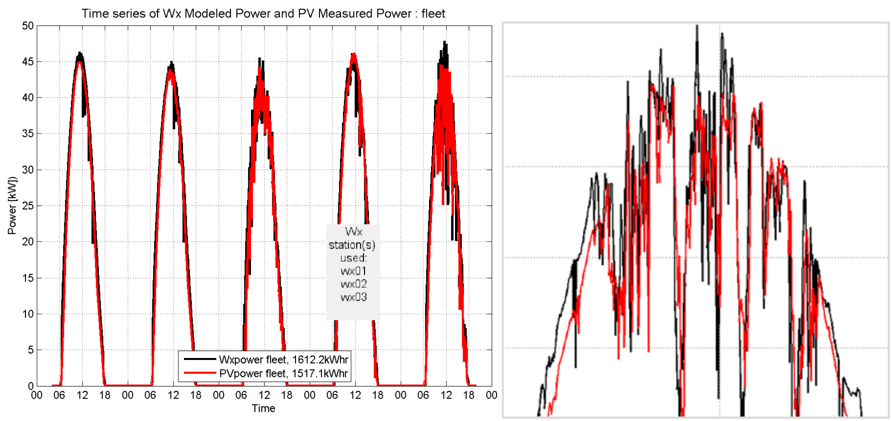

Figure 10. SAM API estimated versus actual production.

4.5.2. Scripting Tools for Spatial and Temporal Visualization

Scripting tools using load shape features of OpenDSS are developed for spatial and temporal visualization of measured and simulated data. The tools are flexible and have a wide range of configurable options. A sample of the results of the visualization tools is shown in Figure 11.

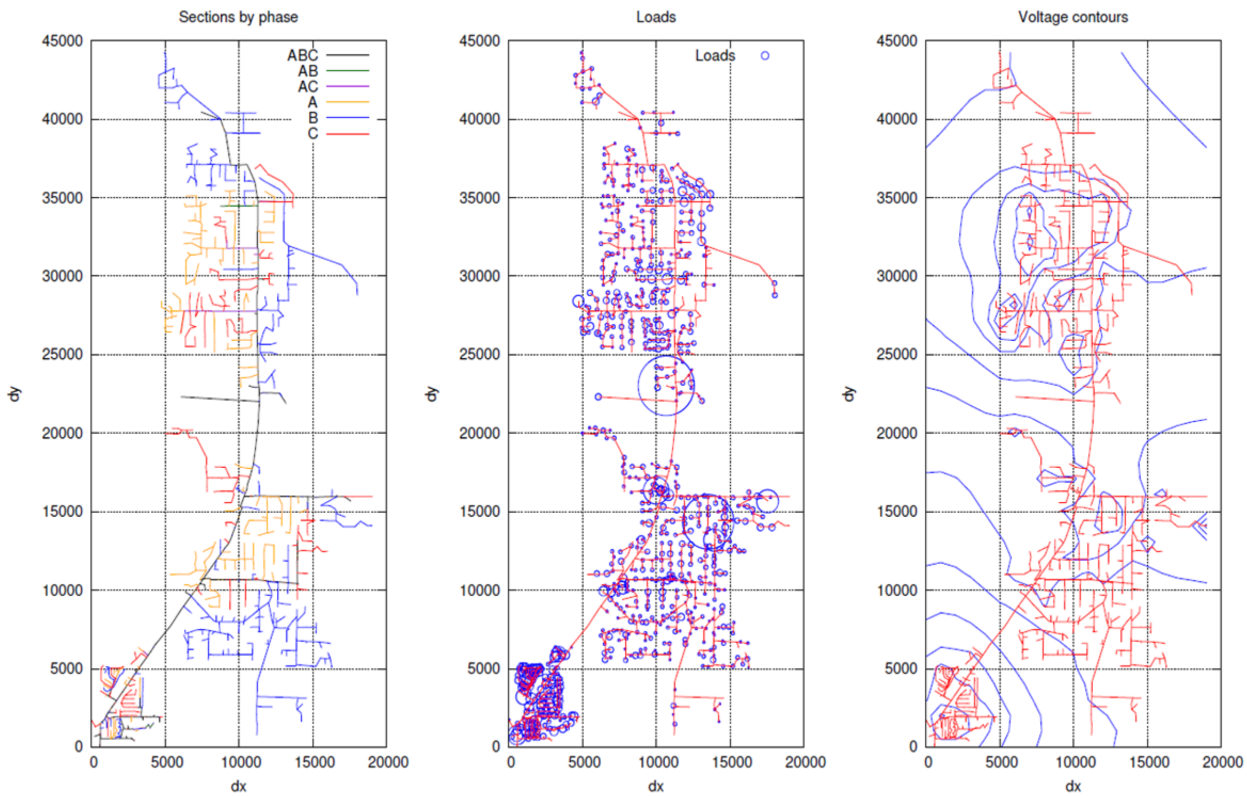

Figure 11. Spatial visualization tool outputs.

4.5.3. *Web Based Visualization*

The web based visualization package using ASP.NET technology consists of live rolling and historic strip charts as shown in Figure 12.

Figure 12. Web based live rolling and historic strip charts.

4.5.4. *NREL Google Earth Tool*

Visualization of real-time production was developed using Google Earth® KML (Keyhole Markup Language). The KML file was generated using real time data and then updated at a desired frame rate and the Google Earth® software is used for visualization.

Visualization Toolkit Key Conclusions

A platform to efficiently store and present relevant information and analysis results is a critical requirement for operations and planning staff. Special consideration must be given to ensure the platform can be scaled to meet additional analysis requirements and that it is integrated into business processes for regular IT maintenance and upgrade as required. Engaging internal IT departments to ensure the platform is constructed using preferred software and hardware tools and methods will provide this assurance.

5. Distribution Modeling and Validation

Models and analytical tools were developed to study the impact of high penetration PV on distribution system operation. These tools were validated and used for two main purposes:

1. Design and analysis tool for high penetration PV distribution feeders
2. Study various what-if scenarios with high penetration PV distribution feeders

In addition to daily patterns, load and PV also exhibit seasonal patterns. Spring, summer, fall, and winter start days were defined based on meteorological or astronomical observations.

Average value load plots showed a two-peak load pattern for each season except summer. A notable increase in summer averages occurs during early afternoon and may be due to air conditioning load. Average winter load was shown to be consistently higher than load in other seasons, possibly due to electric heating. The peak load of the feeder typically happens on a winter evening around 8 PM. The minimum load is around 4 AM but the spring load remains relatively light during most of the sunlight hours. From the standpoint of PV integration, this is an important time interval as the PV production will be at its highest in cool and sunny weather typical of spring mornings.

5.1. Distribution Modeling

The baseline feeder model (Phase I) included all primary conductor segments, transformers, switches and capacitor banks. The detailed high penetration model includes secondary cables, protection devices including transformer and lateral fuses, reclosers and relays, and residential and large-scale PV systems. The loads are modeled using AMI data and are added to the corresponding transformers individually at the meter location. The PV generators are modeled as electronically coupled generators with the active power based on the PV array rating and AMI data. The detailed modeling process was developed in CYMDIST (CYME Distribution System Analysis tool) and the open source OpenDSS (Open Distribution System Simulator).

Using these models, power flow analysis was carried out under different operating conditions including peak load, peak PV penetration, and light load conditions. Protection device coordination, including fuse-fuse, fuse-recloser, fuse-relay, and relay-recloser were modeled and studied. The impact of high PV penetration on the relay sensitivity was also studied.

The modeling process includes the three distinct steps of constructing the corresponding equipment library, building the network model, and creating the load model.

APS provided GIS data, containing transformers, conductors, load data, and PV systems, to create the electrical model of the system. CYMDIST and OpenDSS, two commercially available distribution modeling and simulation software tools were selected and evaluated. OpenDSS was found to have a distinct performance advantage over CYMDIST when running several load flows using scripted runs for arbitrary temporal lengths (for comparison purposes, CYMDIST took more than 11 h for solving 5000 load flows[10], while OpenDSS took less than 5 minutes for the same task).

The feeder network modeling process involves topology identification, secondary lines modeling, transformer and transformer fuse modeling, meter loads allocation and modeling, PV generators allocation and modeling, and protective devices modeling. To

[10] Since this work was initially done, CYMDIST has added modules to streamline this type of analysis

include secondary cables, all sections based on primary and secondary lines and switching cabinets are identified. Nodes are then added based on this identification. MATLAB is used to create the load and network topology TXT files for import into CYMDIST.

In the original GIS data, transformers are represented as a single point. In CYMDIST, the transformers are modeled as a primary and secondary node with fuses.

The GIS data includes 28 types of secondary cables., Unknown cable types were changed to known types based on their phase connections. A standard reference[11] was used to determine the number of strands by matching wire diameters and gauges. Secondary lines are connected to transformer secondary windings. GIS data errors in number of conductors per phase were corrected.

All protective devices have to be modeled to verify device coordination. Protective devices include fuses, reclosers and a substation relay.

Two types of fuses are modeled – primary distribution system protection fuses and transformer fuses (primary and secondary). Solid links are removed. Transformer fuses are independently set per phase.

The two reclosers on SV04 use the fuse clearing strategy and hence the fast curve settings in CYMDIST are set equal to the slow curve settings. The substation multi-relay on SV04 consists of a phase and ground relay, and is modeled with actual relay parameters and trip settings in CYMDIST.

MATLAB scripts connect residential loads to secondary nodes using GIS data or by matching meter numbers. The sum of all connected load data created a spot load section for each node.

Configurable scripting tools evaluate year load-PV cycles using the load-shape feature of OpenDSS. Comprehensive OpenDSS monitor files capture the spatial and temporal results of voltage and power flow.

All PV inverters are modeled as electronically coupled generators of constant active power equal to the PV system rating. The fault currents of PV inverters is typically 2 – 5 times[12] the rated current for 1 to 4.25 ms depending on inverter type and number of phases. Fault contributions of all these PV generators are set to 200% of rated current.

5.1.1. Static Simulations of Peak Load and Peak Penetration

Power flow using the extended CYMDIST feeder model, with and without PV under different operating conditions was simulated. AMI meter and PV data Jan 1, 2014 to September 30, 2014 are used to determine highest load and highest penetration cases for simulation. The voltage at the feeder head is measured and used in the simulations, and load power factor is set to 0.89.

---

[11] T.A. Short, 'Electric Power Distribution Handbook,' CRC Press, September 2003

[12] J.Keller, B.Kroposki, *'Understanding Fault Characteristics of Inverter-Based Distributed Energy Resources'*, NREL/TP-550-46698, January 2010

The highest load value modeled occurred at 8 PM on Jan 5, 2014 (116th hour), with zero PV generation. The substation voltage is measured and simulated as 1.028 pu.. The operating conditions corresponding to the highest load case are given in Table 5. PV generation is negligible due to low insolation at the late evening hour in winter. Transformer no-load losses are not modeled.

Table 5. Highest Load Operating Parameters

Parameter	kW	kVAr
Total load	5484.26	2707.20
Total PV generation	0	0
Total losses (obtained from simulation)	176.76	359.78

Since PV generation is negligible, it does not affect the voltage, kW, and kVAr profiles along the feeder. The capacitor banks cause kVAr jumps, and their effects are also seen on the slope of voltage profiles. The voltage at the feeder-end is within ANSI limits. If the DPRES and Cromer PV plants are set to provide maximum reactive power support (90% of rated kVA), the feeder voltage can be supported to be within ANSI limit even with the two voltage controlled capacitor banks turned off, i.e., the larger inverters can potentially reduce the requirements on capacitor banks or reduce the number of operations.

The highest PV penetration (41.97%) occurred at 12 PM on March 24, 2014 (2004th hour), with substation voltage measured and simulated as 1.028 pu., and the operating parameters are given in Table 6.

Table 6. Highest Penetration Operating Parameters

Parameter	kW	kVAR
Total load	2977.81	1508.89
Total PV generation	1249.81	0
Total losses (obtained from simulation)	32.56	49.31

Losses are significantly lower than Table 5 due to PV reducing power flow from the substation. The feeder load flow profiles are simulated with and without PV in order to understand the impact of increasing penetration. The losses in Table 6 increase to 64.59 kW without PV. PV improves the voltage profile with feeder end voltage drop reduced to 0.0047 pu from 0.021 pu with no over voltage on any primary node. Capacitor banks remain on. PV causes step decreases in real power, with reverse power flow at DPRES and Cromer. Since this reverse power flows through one of the feeder reclosers, anti-islanding schemes have to be carefully evaluated for situations when this recloser is opened.

The baseline PV performance (active power only) was analyzed using data from Aug 05, 2012 through Aug 11, 2012 from the substation and feeder DAS.

On weekdays, substation load is cyclical with one peak and two valleys. While one of the valleys is due to low demand at midnight, the mid-day valley may correspond to PV generation. Reverse power flow occurs at a particular feeder location (fdrDAS4) during peak PV production. There is a strong correlation of POI voltage at DPRES with active and reactive power output from the inverter.

5.1.2. Quasi Static Time Series Simulations

Quasi steady state time series modeling was used to study the impact of system variation over time. Studies may include impact of clouds or control properties of capacitor banks. OpenDSS is used for all time-series simulations. PV, feeder DAS, and AMI hourly data are imported into OpenDSS using scripts, and repeated load flow simulations are run over specific time periods. The base model without secondary lines was used for the simulation. Monitored simulation results were compared to actual measurements.

To properly model substation voltage fluctuations, the substation DAS measurements were used to model the substation voltage in OpenDSS. This was accomplished by adding another voltage source with low series impedance near the substation with field measurements provided time-series values. The voltage source values are controlled via the OpenDSS COM interface using MATLAB.

The errors in the simulated feeder voltage magnitudes compared to the corresponding field measurement were within 2% giving good confidence in the models and methods developed. Better field data on the kVAR measurements and capacitor bank operations will help to further improve the matching of simulation and field measurements.

5.1.3. Modeling Data Resources

The modeling process is outlined in Figure 13. Accurate models require detailed information which can prove to be difficult to obtain. The required information includes GIS data which give locations and basic information (e.g. equipment type, rating, etc) for lines and equipment on the feeder, system equivalent impedance at the substation, transformer impedance data, load data, PV generation data, voltage data at the feeder head, utility construction standards for line conductors and spacing, and in-field measurements for model validation. Some parameters had to be calculated based on engineering texts where no data existed. The feeder data is also in constant flux as customers move on or off the feeder, or as equipment is upgraded or retired. During the course of the study, the GIS system underwent several revisions. All these changes create challenges for accurate modeling and validation.

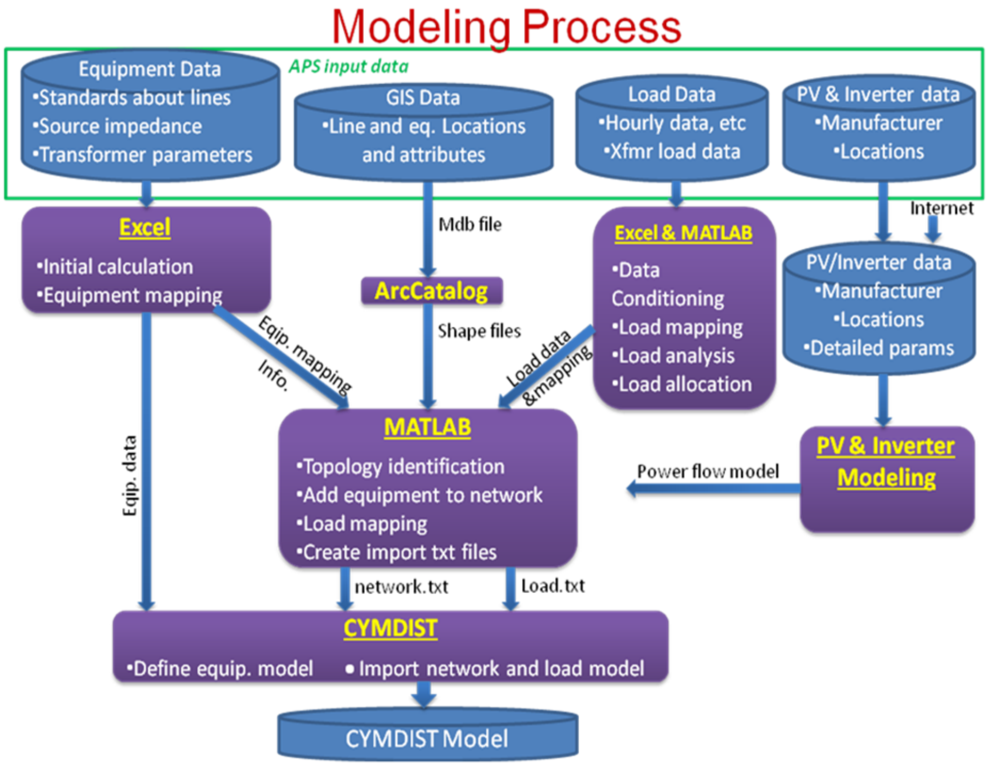

Figure 13. Modeling process flow chart.

5.2. Model Validation

Phase I developed a data acquisition context to support the study. The requirements capture data variables to validate models, and to operate and maintain the PV systems and related hardware for the duration of the study and beyond.

To validate the steady state model, three parameters are reconciled: active power, reactive power, and voltage. Measured values are compared against model results at specific locations on the feeder corresponding to feeder DAS or residential PV DAS sites.

One-minute feeder and PV DAS measurements are used for validation. One-second weather data is used to predict PV output. One-hour and 15-minute AMI data is used for load and PV output allocation. Since some meter data are not included in the AMI database, to improve accuracy and temporal resolution, the zone allocation method was developed for quasi-steady state modeling, as well as steady state model validation.

Snapshot simulations in CYMDIST for the highest penetration (12 PM, March 24, 2014) and highest load (8 PM, January 5, 2014) cases are compared with DAS measurements. The results of the highest penetration scenario are presented in Table 7. Maximum error was under 3%. Table 7 includes simulated secondary voltages in addition to simulated and measured PV voltages.

Table 7. Steady State Model Validation for Highest Penetration Case

PV DAS ID	Measured PV Voltage (V)	Simulated PV Voltage (V)	Error (%)
PV DAS01	122.92	123.38	0.37
PV DAS02	122.88	124.35	1.20
PV DAS03	123.64	124.49	0.69
PV DAS04	123.33	123.71	0.31
PV DAS05	122.98	123.7	0.59
PV DAS06	124.29	123.27	0.82
PV DAS07	124.55	123.46	0.88
PV DAS08	123.34	123.33	0.01
PV DAS09	124.18	124.3	0.10
PV DAS10	123.68	125	1.07
PV DAS11	123.63	124.93	1.05
PV DAS12	123.37	124.05	0.55
PV DAS14	123.68	124.66	0.79
PV DAS15	123.49	124.01	0.42
PV DAS16	124.05	124.12	0.06
PV DAS17	288.40	279.97	2.92
	286.95	281.38	1.94
	288.98	283.23	1.99
PV DAS18	7482.46	7401	1.09
	7477.83	7454.38	0.31
	7495.20	7491.77	0.05

Quasi, steady-state model validation was performed with one-minute data and simulation for September 25, 2012 and with one-hour data and simulation from September 25, 2012 to October 24, 2012. Simulation results at each DAS location is compared to measured DAS and AMI data.

Comparison of one-minute measured and simulated voltage at DAS05 is shown in Figure 14. The rms deviations in voltage are less than 2%. One-minute measured and simulated data for DAS05 are shown in Figure 15 for kW and Figure 16 shows the kVAR comparison at the substation. Since load allocation is based on DAS measurements, the kW values match within 5% as expected. Jumps in kVAR values are due to capacitor bank switching. If the capacitor bank switching times are matched in measurement and simulation, the kVAR values match within an acceptable margin.

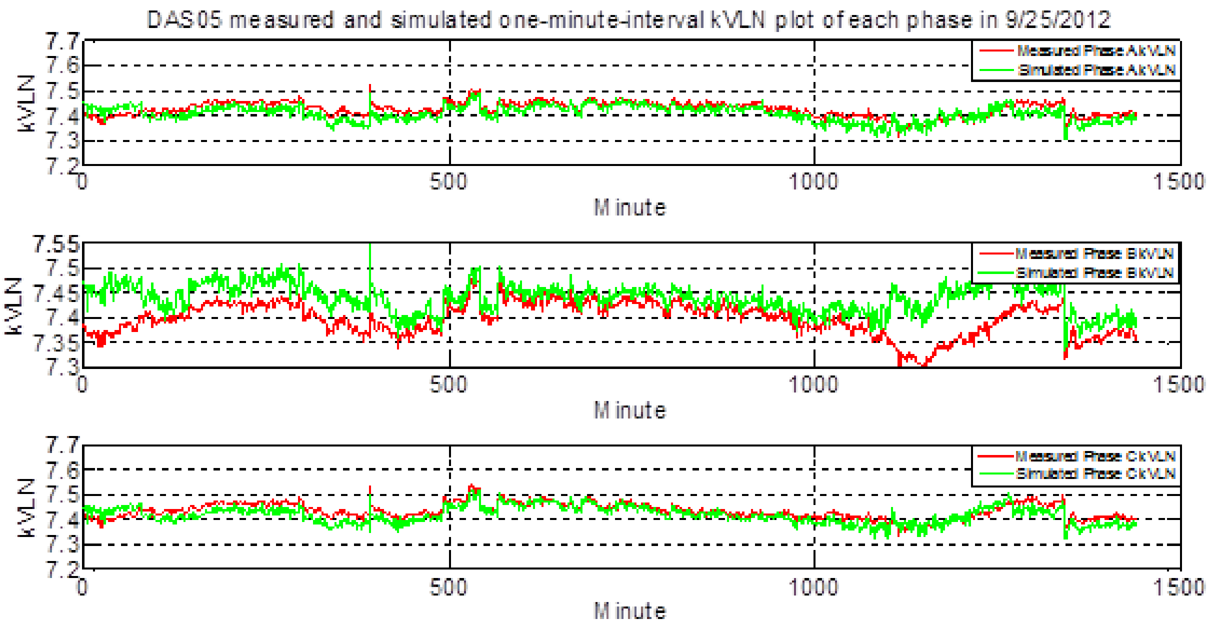

Figure 14. One-minute voltage data validation @ DAS05.

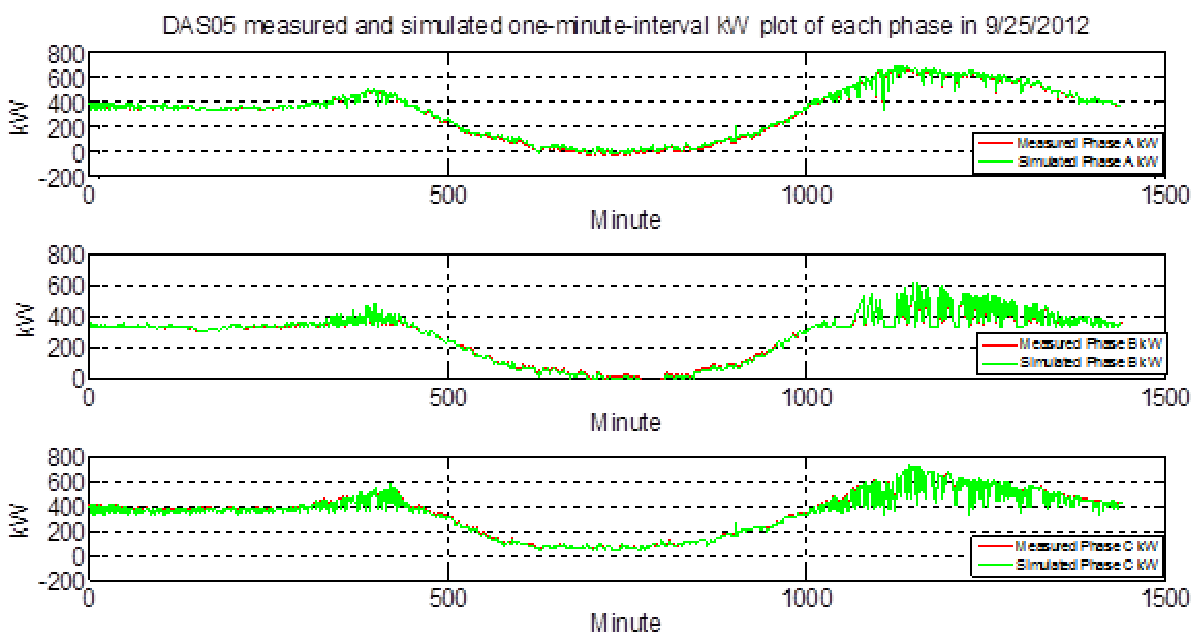

Figure 15. One-minute kW data validation @ DAS05.

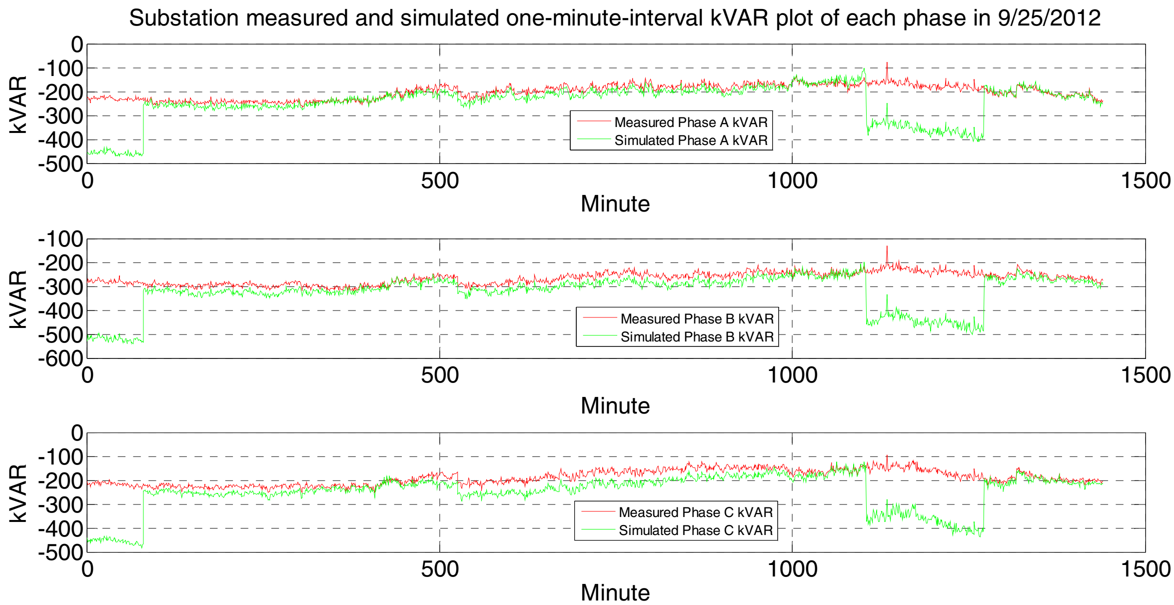

Figure 16. One-minute kVAR data validation @ substation.

One-hour data validation was performed by averaging the load data for each hour. Simulated and measured voltages are matched within 1% and the plot of measured and simulated voltages at DAS05 is given in Figure 17.

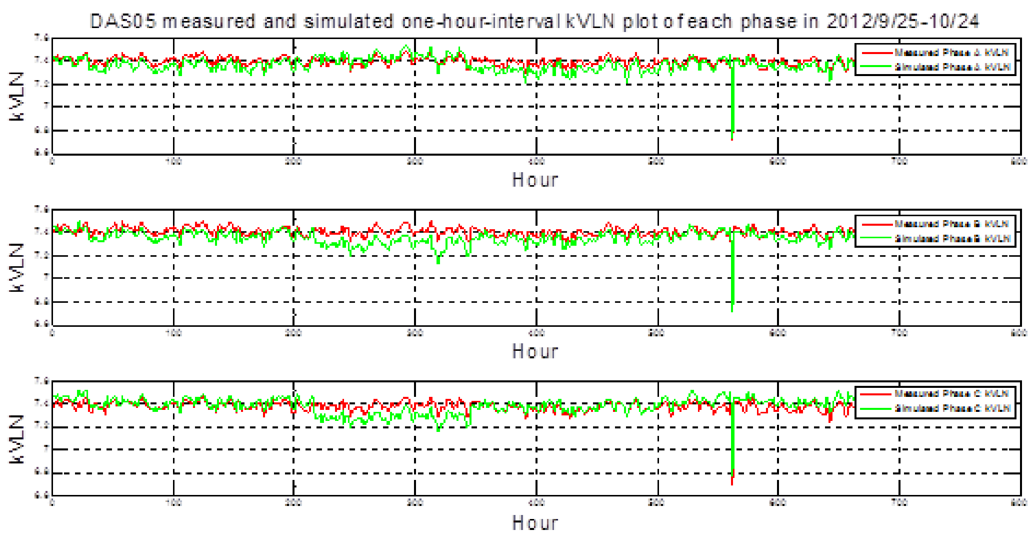

Figure 17. One-hour voltage data validation @ DAS05.

5.3. Feeder Reconfiguration

Feeder reconfiguration is a typical utility process that must be considered as part of any high penetration distribution feeder modeling exercise. The Sandvig 10 (SV10) feeder in Flagstaff is adjacent to SV04. APS's EMS (Energy Management System) recorded a reconfiguration event in September 2012 (Figure 18). OpenDSS was used to recreate this event in software simulation and perform analysis. QSTS tools are used for simulations. Since SV10 PV data lacked detailed measurements and information, , SV04 PV data were used as a baseline for assumptions on SV10.

Figure 18. EMS data showing reconfiguration event on SV04 and SV10.

5.3.1. Baseline without Reconfiguration

A baseline simulation, without reconfiguration, was performed to validate the simulation method. Capacitor banks in SV04 and SV10 are assumed to be in local control. ANSI voltage violations are shown in Figure 19. This simulation was based on partial AMI and limited PV system data.

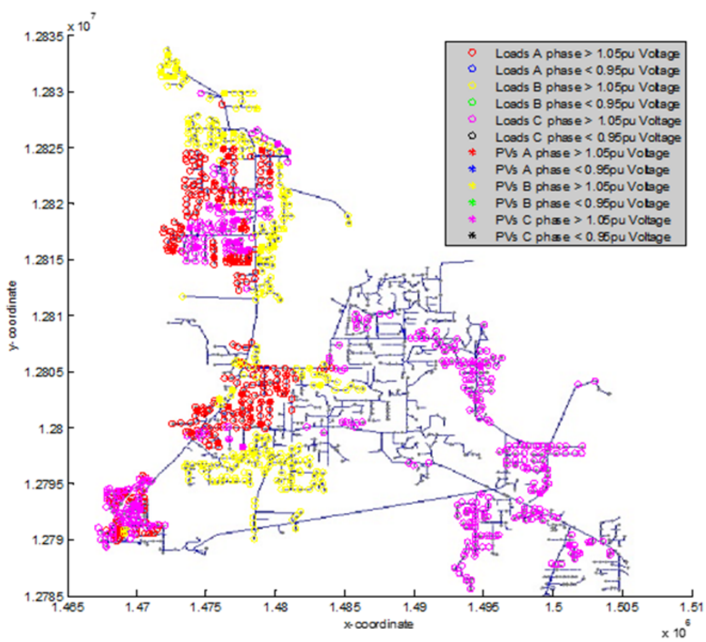

Figure 19. ANSI voltage violations for baseline without reconfiguration.

5.3.2. Reconfiguration of SV04 and SV10

SV10 is connected to SV04 using the farthest (north-east) tie-in point from the SV04 feeder head. With capacitor banks set to local controls, the solution did not converge. To achieve convergence, all capacitor banks in SV10 are turned on and all capacitor banks on SV04 are turned off, since SV10 ties to the middle of SV04. The ANSI violations are shown in Figure 20, with several low voltage nodes in SV10. In this analysis, incomplete information has a detrimental effect on modeled results. To improve the accuracy of QSTS simulations, the operation of the capacitor banks have to be modeled accurately. AMI information for the base model has to be refined and complete AMI data needs to be obtained for the period of time under study. Regardless of absolute voltage magnitudes, it can be seen that voltage at specific locations may be affected.

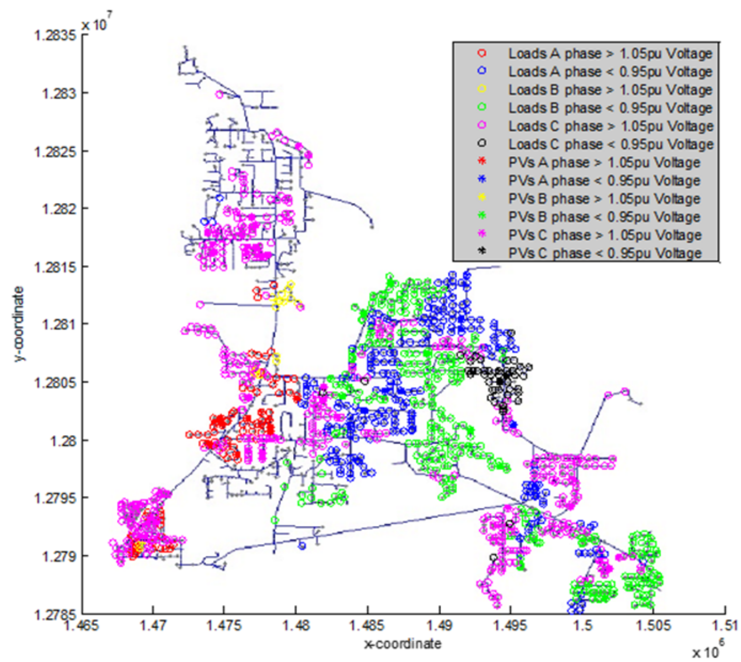

Figure 20. ANSI voltage violations after reconfiguration.

6. Strategies for increasing PV hosting capacity

Strategies for increasing PV hosting capacity were explored through demonstration and modeling. These strategies include traditional approaches like feeder re-conductoring and other emerging options like grid support inverters and energy storage.

6.1. Grid Support Inverter Demonstration

Modern PV inverters, in addition to delivering PV energy to the grid, must act to control power delivery to meet utility concerns such as anti-islanding, prevent back feed into a fault, provide voltage and frequency range protection, limit harmonics, and provide DC injection protection. PV inverters can also provide reactive power to prevent/mitigate high-penetration issues like voltage fluctuation.

At the time of field commissioning, the GE inverter was one of the few manufacturers with a UL-listed inverter with grid support functionality. GE's product development team had already developed and tested the modes and controls described below. This project gave the team opportunity to demonstrate these modes on a working utility feeder.

The GE Brilliance® and SunIQ® system were installed and commissioned at DPRES. The SunIQ data acquisition features provided the capability to trend and store multiple variables over extended periods of time. Figure 21 shows the inverter irradiance, power, and voltage for one week. Duration 1 and 2 show that voltage fluctuations can happen during both a clear and cloudy day, while duration 2 shows a smoother voltage profile during a cloudy day. Hence, the feeder point of interconnection is too stiff to be significantly affected by the 600 kW PV installation.

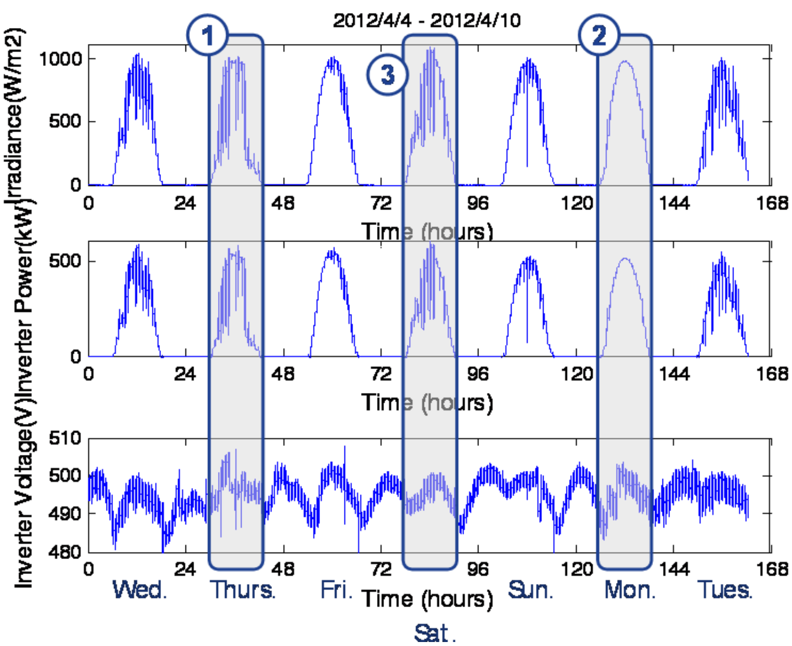

Figure 21. Doney Park inverter irradiance, power, and voltage over one week.

The short circuit ratio (SCR) for DPRES was determined to be 43.8, which is a strong grid connection. GE derived a simple impedance model for the inverter from the distribution feeder model. Point of interconnection (POI) voltage fluctuation can then be derived from approximate voltage variations due to active and reactive power flow. The simple model shows that 100 kVA of excess rating will allow approximately 1.1% voltage regulation, while the entire capacity (nighttime) will allow approximately 2% voltage regulation.

APS finalized the PV plant interconnection methodology and requirements at DPRES, including the advanced grid support features. GE installed its Brilliance solar inverter at APS's Doney Park site. Installation of the inverter allowed APS and GE to develop and document utility practices for solar inverter installation and operation. Additionally, techniques were identified and implemented allowing SCADA integration with utility (APS) and inverter operator (GE) access while maintaining cyber security. GE believes both of these results will help to advance acceptance of utility scale solar.

APS cyber-security requirements resulted in delays to integrate the SunIQ with APS's historian. Alternate options for data collection and plant control were developed to satisfy both APS and GE standard operating procedures. GE retained static TCP/IP connectivity over a 3G modem, while APS received either a Modbus or DNP3 over serial data stream. A commercial OPC package (MatrikonOPC®) was used to convert GE's OPC data stream to Modbus over serial. The Modbus signal is read by an APS data concentrator (SEL™ RTAC) for storage into APS historian (OSISoft PI®).

The inverter was operated in multiple control modes, including active power mode, power factor mode, and voltage control mode. GE's new voltage control mode was also tested and compared with traditional methods. Field data from deployed DAS and the SunIQ system were analyzed to develop analysis tools and verify new modes of inverter operation.

Ramp rates of inverter power and POI voltage are used as performance metrics for PV variability. Rolling averages are used to filter high frequency noise. Ramp rates are the difference between two consecutive averages. A simplified equivalent circuit with the inverter connected to a step up transformer in series with the feeder impedance is used for voltage variation analysis. MATLAB scripts determine major and minor ramp rates and capacitor bank operation events.

Figure 22 shows the voltage, real, and reactive power at the POI with time steps of 20s, 40s, and 60s. Red bands cover data with less than 1% power variations, and blue bands greater than 1%. The ΔP-ΔV plot shows voltage sensitivity to real power and the ΔP-ΔQ plots show reactive power sensitivity to active power changes. The width of the blue bands (ΔP) at 20s shows solar intermittency and depends on feeder impedance and active/reactive power injection. The red band corresponds to uncorrelated operations such as cap bank switching and load changes. The application of advanced controls to reduce the uncorrelated variations in voltage will help reduce the size of the red bands.

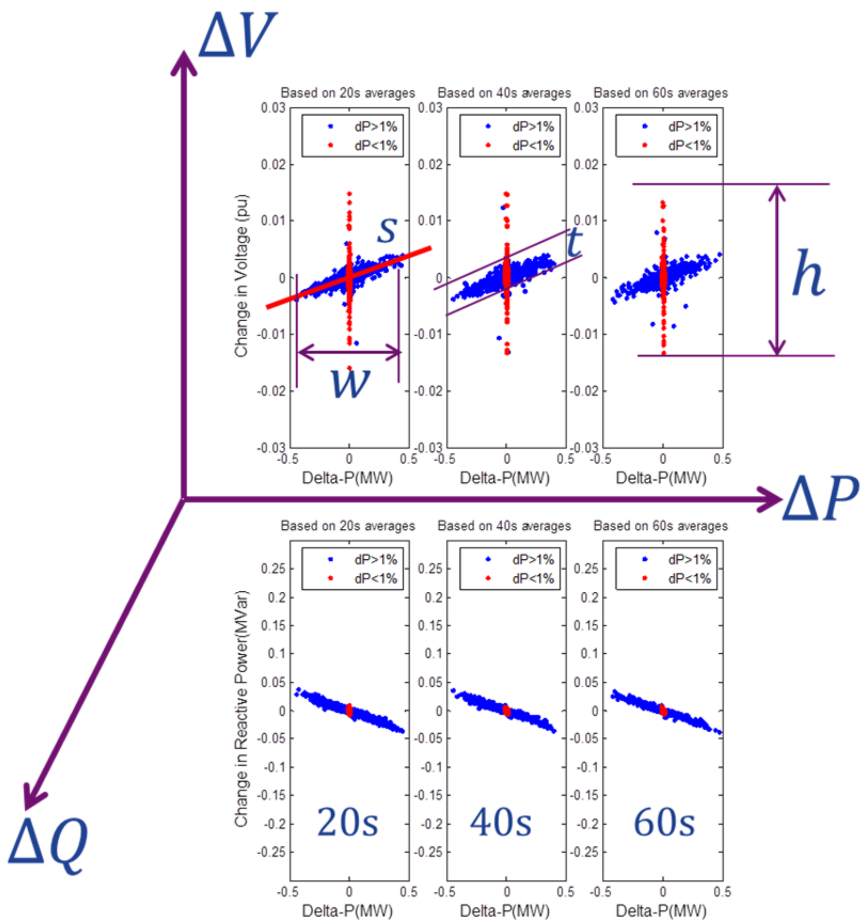

Figure 22. Correlations between voltage, active power and reactive power at POI.

The advanced grid support features of the GE inverter were enabled under different experimental modes. The inverter was operated under each mode for at least a week. Operational data was collected and analyzed.

In the voltage control mode the inverter regulates the voltage by injecting or absorbing reactive power. The performance results are shown in Figure 23. Voltage variation is stable and near zero. Some voltage sags and swells are observed due to reactive power curtailment. Active and reactive powers are not closely coupled.

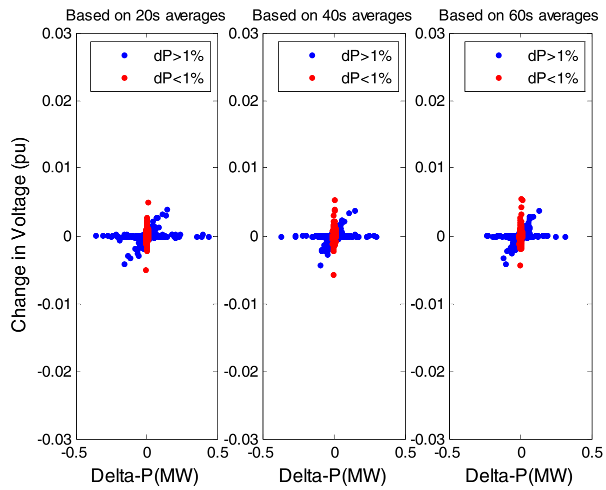

Figure 23. Voltage ramp events in voltage control mode.

In the active power control mode, the inverter injects active power into the grid. The measured performance results are shown in Figure 24. The interconnection transformer causes small negative reactive power flow. Control loop dynamics cause rapid changes in reactive power. Changes in active power are positively correlated to voltage variations.

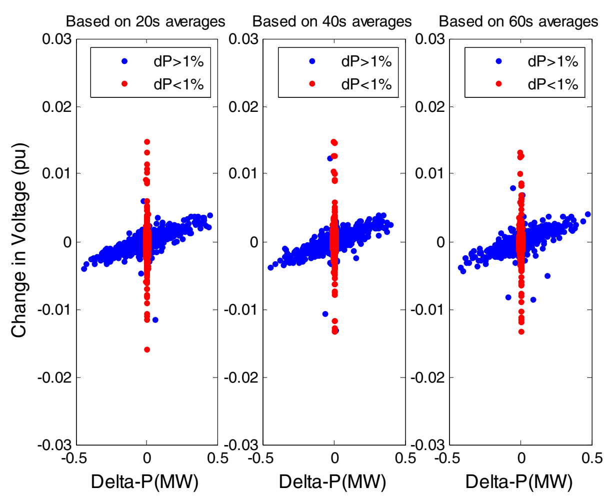

Figure 24. Voltage ramp events in active power mode.

In power factor mode, the inverter maintains the real to reactive power ratio. The performance is shown in Figure 25. The injected reactive power in this mode is higher than active power mode. Voltage variation is reduced, and real power is negatively correlated to voltage. Real and reactive powers are strongly correlated.

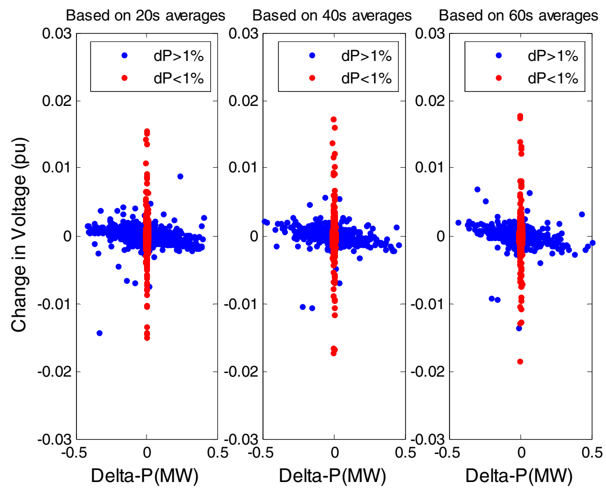

Figure 25. Voltage ramp events in power factor mode.

In the reactive power mode, the inverter absorbs a fixed amount of reactive power. The performance results are shown in Figure 26. Control loop dynamics cause rapid reactive power changes. Voltage variations are positively correlated to power. The control loop decouples active and reactive power leading to a weak correlation.

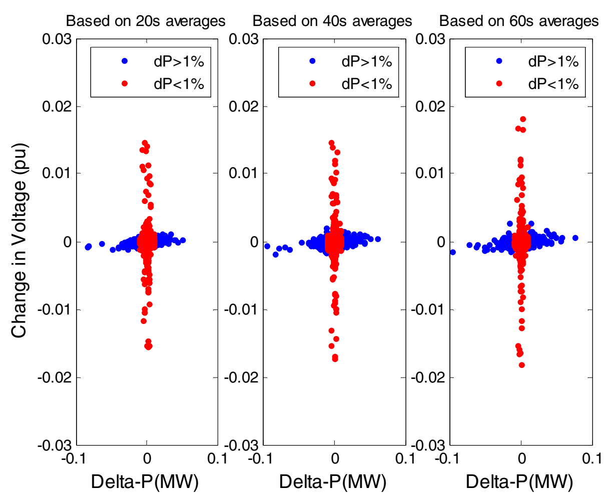

Figure 26. Voltage ramp events versus active power in reactive power mode.

- In active and reactive power mode, voltage has a positive correlation with active power.
- In active and reactive power mode, reactive power is relatively independent of real power.
- In power factor mode, voltage is less sensitive to real power. Reactive power is dependent of real power.
- In the voltage mode, the voltage is relatively stable, while the reactive power changes rapidly, which could exceed reactive power capabilities.
- In conjunction with each inverter control mode, the active power output of the inverter can be curtailed. The power can be curtailed using a controlled slew

rate. Recovering from curtailment takes longer by design to lower impact on POI voltage. Stepped active power curtailment is also possible.

GE developed a new voltage control mode, tested it under the RTDS environment and implemented it into the GE Brilliance Inverter. This new mode allows voltage to vary naturally and also allows other feeder voltage regulating devices to be largely ignored. However, it regulates voltage at the POI for solar intermittency. The new mode may also be used to dampen voltage fluctuations caused by other installations or load variations.

The new mode provides for a slower smoothing of the voltage. The reactive power requirements for the new mode are shown in Figure 27.

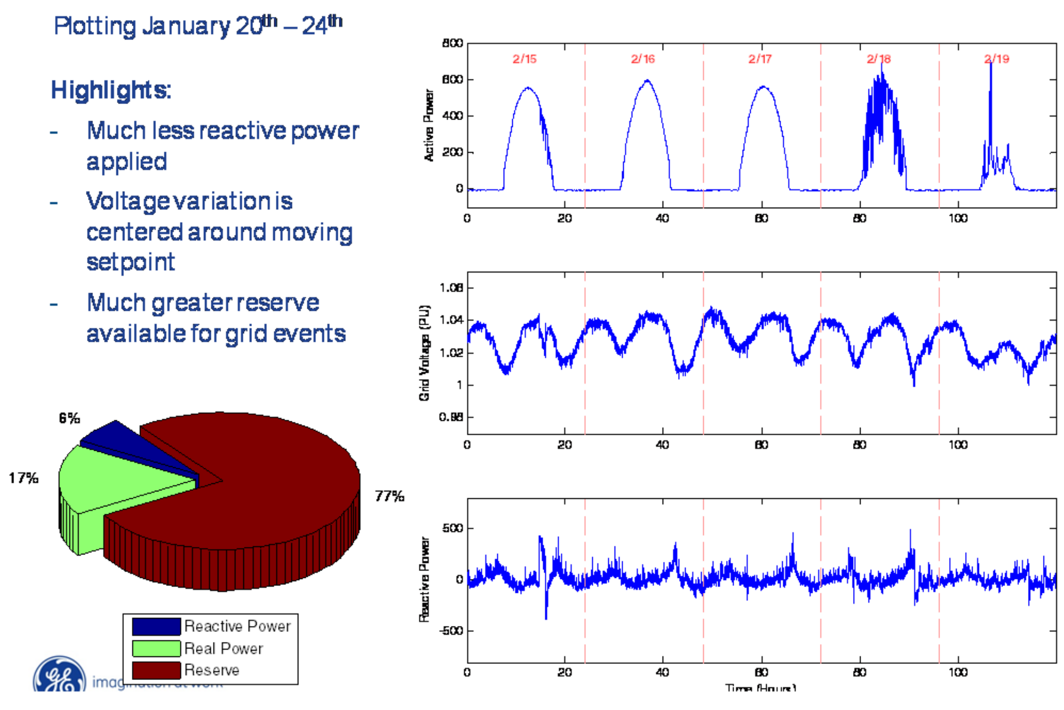

Figure 27. New voltage control mode reactive power injection.

After the various inverter control modes were successfully tested, a SCADA system was deployed to control the GE Brilliance inverter at DPRES. These control modes can allow APS to exercise smart inverter modes for feeder-wide optimization and accommodate grid situations that are not visible to SunIQ and the inverter control loop.

Table 8 gives GE's recommended control modes for grid support inverter operation.

In the case of Doney Park, the inverter can be left in active power mode, without adverse effect on the distribution network. If voltage stability is desired, operating in the power factor or new voltage control mode is recommended. As seasonal variations occur, setpoints can be changed to achieve optimal operation.

Table 8. Recommended Advanced Grid Support Modes.

Operating Conditions/Goals	Active Power	Power Factor	Static VAR	Traditional Voltage Control	New Voltage Control
Doney Park – as of 6/1/2013	✓	✓			✓
Single mid-sized solar installation with a strong grid connection (less than +/- 5% influence on grid voltage)	✓	✓			✓
Single large solar installation with a strong grid connection (greater than +/- 5% influence on grid voltage)		✓			
Single mid-sized or larger solar installation without a strong grid connection					✓
Compensation for local constant reactive power source/load			✓		
Feeders without existing voltage regulation				✓	
Low interaction with existing voltage regulation	✓	✓			✓
Feeders with rapid voltage swings from distributed generation or variable loads				✓	✓
Low maintenance operation	✓				✓
Low reactive power injection	✓	✓			✓

6.2. Energy storage

Energy storage as a mitigation strategy was modeled in OpenDSS. Energy storage was modeled as a generator that can be a source (discharging) or load (charging) that can act independently or externally controlled. The ESS (Energy Storage System) can also be set to idle. Charge, discharge, and idling losses can be specified. The model supports multiple dispatch modes: follow, external, load level, and price. The follow mode was used for simulation where real and reactive powers are preloaded.

6.2.1. Validation of Feeder Model with ESS at DPRES

Details of the ESS at DPRES are given in Table 9. Charge and discharge are controlled by settable triggers based on loads and cycles. Typical simulation results for a typical weekday in September are shown in Figure 28. The charge-discharge cycle of the ESS is shown, along with power drawn from the grid and voltage on phase A at DPRES, before and after applying energy storage.

Table 9. Modeled Energy Storage System Specifications

Parameter	Value
Active power limit	500kW+/-
Reactive power limit	400kVAr+/-
Speed of response	step response (0%-100%) in 30ms-40ms
Switching frequency	2kHz
Efficiency	>97%
Overload capability	10 min 120% 30 sec 150% 2 sec 200%
Charging and discharging efficiency	90%

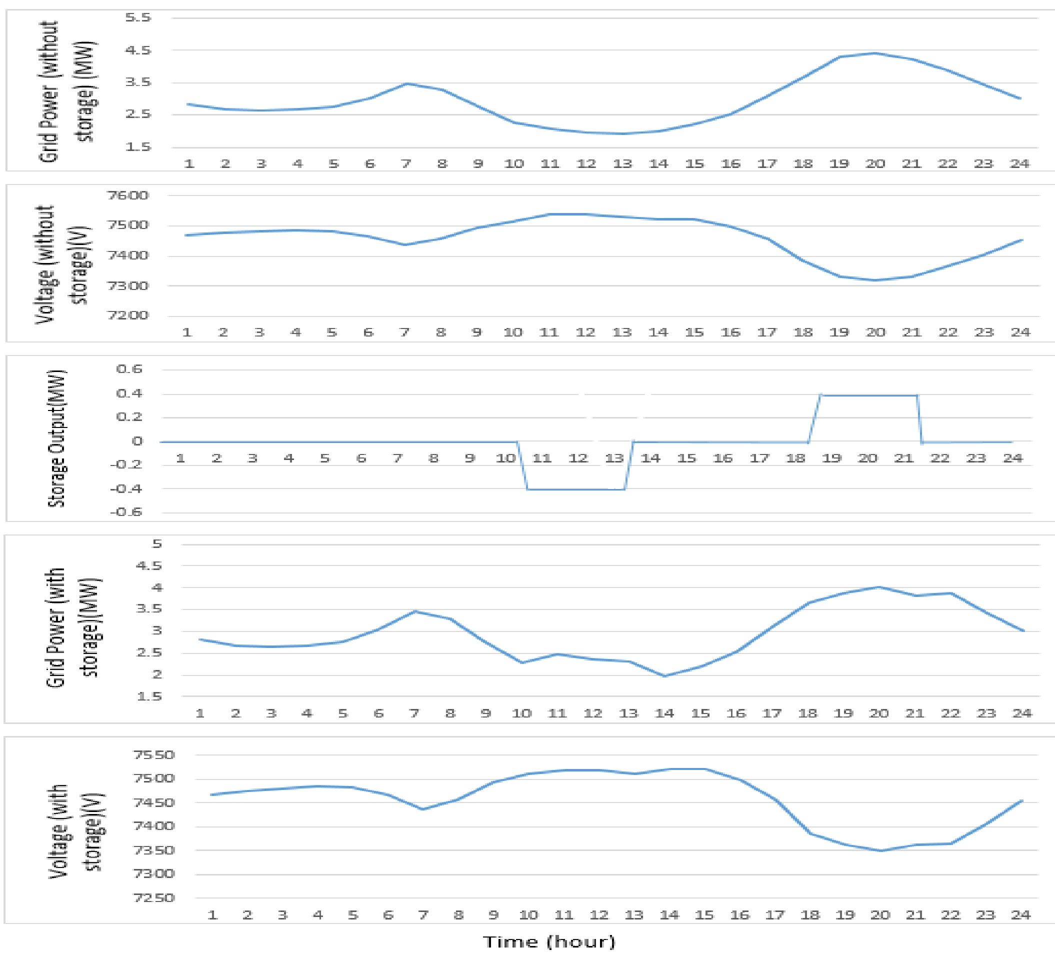

Figure 28. ESS simulation results for typical September weekday

6.2.2. *Optimal Sizing, Planning, Allocation, and Dispatch of ESS*

Energy storage was modeled to improve feeder operation by mitigating uncertainty due to PV variability and for load shifting. First, energy storage is sized by the power and energy imbalance obtained by OpenDSS time-series simulations. Once the total size of ESS is determined, different objectives (as listed in Table 10) are considered in optimization models for allocating (placement) and operating (scheduling) the ESS. Choosing different objective functions raises different computational complexities. Thus optimization tools (Table 10) are selected carefully according to the chosen objectives.

Table 10. Energy Storage Optimization Objectives and Tools

Model	Objective	Computational complexity	Modeling language	Solver
1	Minimizing the deviation of the voltage profile	high	AMPL (commercial)	KNITRO (commercial)
2	Minimizing operational cost or active power losses (with voltage profile as rigid constraint)	Low	MATLAB (through YALMIP)	SDPT3/SeDuMi (free)

6.2.3. *Support of High Penetration*

To support high PV penetration, energy storage is used to increase load during low-load, high-PV instances to lower voltage rise. This application of ESS can be regarded as time shifting of PV or load. For SV04, PV capacity is increased in simulation until an ANSI voltage limit is first violated in at least one node. This value of PV capacity is considered the base hosting capacity, i.e., hosting capacity without any mitigation measures. Simulation results show that for SV04, the base hosting capacity is around 150% of the rated capacity of all the existing PV installations. The ESS power rating and energy rating are then determined so that voltage limits are brought within ANSI limits for different levels of PV capacity

Table 11 (Case 1) shows the requirements on ESS power and energy ratings to increase the hosting capacity by 15%, 25%, 50% and 100% respectively above the base hosting capacity.

As an effective reactive power source, the smart inverter is considered to be combined with ESS for supporting high PV penetration. In this part of the study only the reactive power support from the two large PV plants – Doney park and commercial PV site, is considered. With smart inverters at both these PV plant locations, the required ratings of ESS for improving the PV capacity by 15%, 25%, 50% and 100% above the base hosting capacity are listed in Table 11 (Case 2) respectively.

Table 11. Energy Storage Simulation for Higher PV Hosting

Percentage of improvement	Case 1: without smart inverter		Case 2: with smart inverters at the commercial PV plant locations	
	Power rating (kW)	Energy rating (kWh)	Power rating (kW)	Energy rating (kWh)
15	349	516	349	433
25	561	1139	561	686
50	1082	3524	1082	1730
100	2128	9999	2128	3826

Since the reactive power capability of the inverters is limited during high peaks (in Table 10 the kVA rating is considered to be equal to the maximum kW rating), the smart inverter is not able to mitigate the voltage violations. This is the reason why combining smart inverters cannot reduce the required power rating of ESS. However, the durations of the voltage violations are significantly reduced, so the required energy rating of ESS is also reduced. To validate this conclusion, four cases are studied for voltage violations due to high penetration: without smart inverters, with a smart inverter at DPRES, with a smart inverter at the commercial PV site (Cromer), and with smart inverters at both sites. Results of the simulations with the inverters providing maximum possible reactive power (considering the kVA rating and kW injected) are shown in Figure 29.

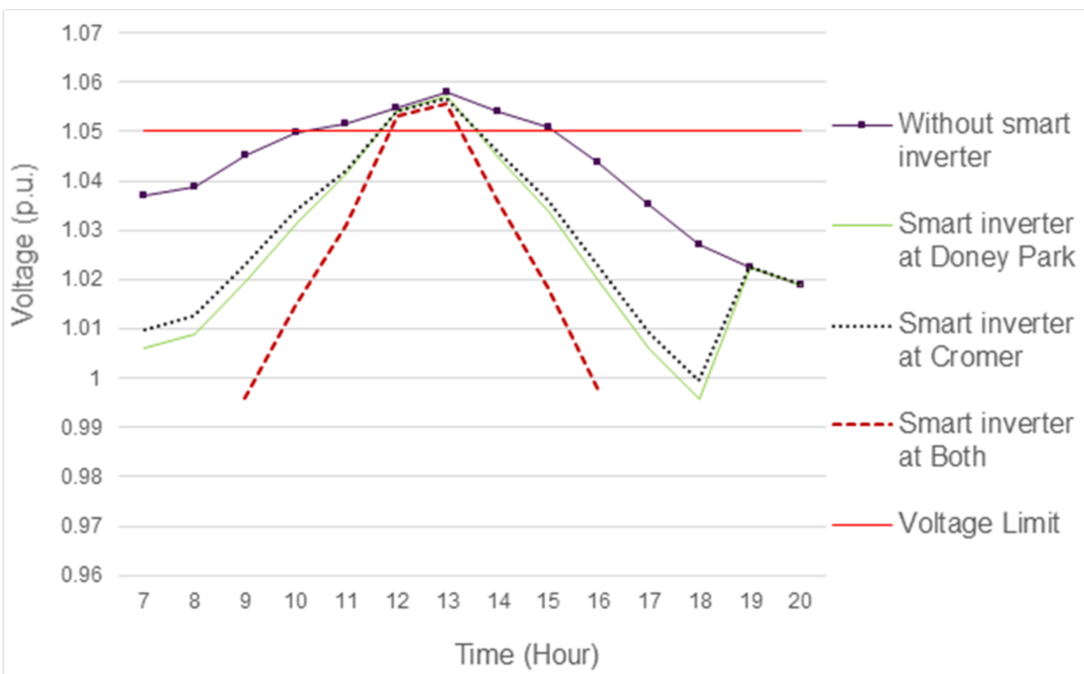

Figure 29. Worst case voltage violations on SV04 under high penetration.

When PV capacity is set to 200% of the installed rating (33% higher than the base hosting capacity), the required ESS power rating is obtained as 0.7 MW for 4 hours. The above ESS is then optimally allotted among different potential locations on the feeder using a simplified model with pre-chosen locations (Figure 30).

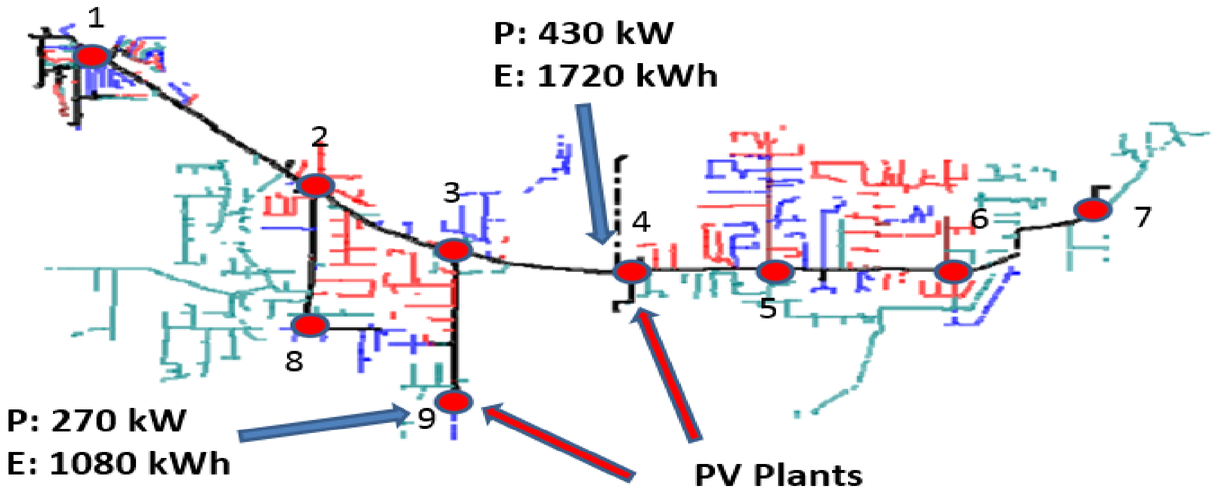

Figure 30 Optimal allocation of ESS for SV04.

Dispatch is then optimized to minimize voltage variation. Figure 31 shows that optimal ESS charging is obtained by tracking PV generation, and optimal ESS discharging (Figure 32) by tracking heavy loads.

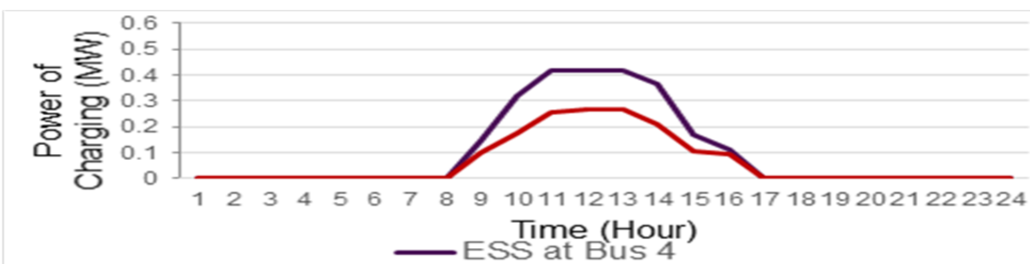

Figure 31. Optimal charging pattern.

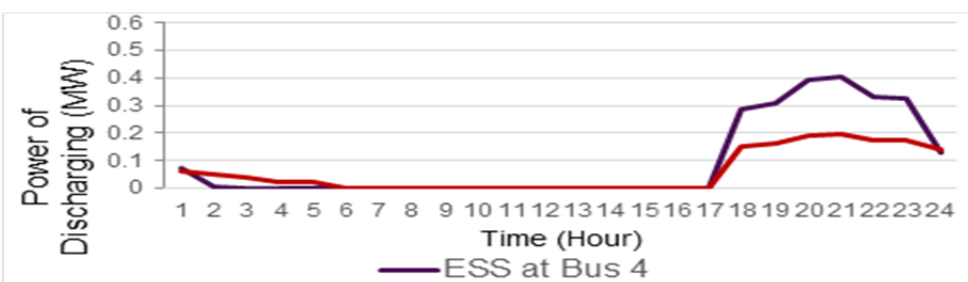

Figure 32. Optimal discharge pattern.

In the scenario described above, with double the original current levels, time series simulation in OpenDSS shows voltage violations of upper ANSI limits under high PV penetration without ESS. With optimal ESS allocation and dispatch of the above ESS, voltage returns within the ANSI limits. Without ESS, at SV04, ANSI limits are violated at 50% penetration and ESS should be considered if penetration approaches 50%.

Analyses were also carried out with the inverters having higher kVA capacity such that large reactive power can be absorbed even at rated active power injection. The results show that with roughly 10% higher kVA capacity (corresponds to reactive power capacity of about 46% of kW rating) while injecting full rated active power, ESS would not be required to mitigate voltage violation at the higher penetration levels.

6.2.4. Mitigating PV Uncertainty Caused by Cloud Cover

The effect of cloud cover on PV generation and the simulated voltage profile in a high penetration scenario are shown in Figure 33. The objective of the smart inverter-energy storage combination is to mitigate the fast power and voltage variations caused by cloud cover.

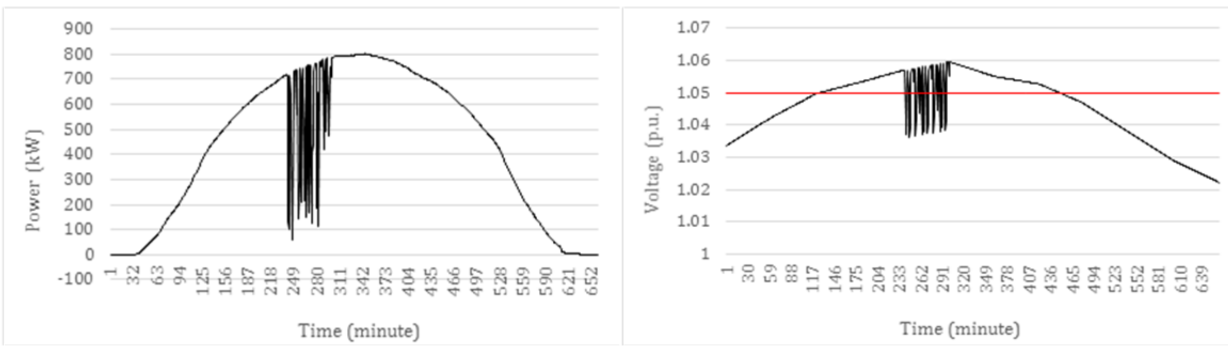

Figure 33. PV power and voltage profile of a PV plant with high penetration.

To avoid over-sizing, the size of energy storage was determined using errors (differences) in measured and forecast power and energy from the PV plant. The differences are calculated for each hour of the day for a year and daily maximums are used to obtain a statistical cumulative distribution function of the power error and energy error. Then, given a desired power error distribution (*p%*) and energy error distribution (*e%*), the value of the maximum power and energy can be determined from the cumulative distribution functions. These give the power rating and the energy capacity of the ESS. The ESS can then mitigate daily power error in *p%* of cases and daily energy error in *e%* of cases. This sizing procedure was implemented in MATLAB and verified using field data from the commercial PV site and Doney Park.

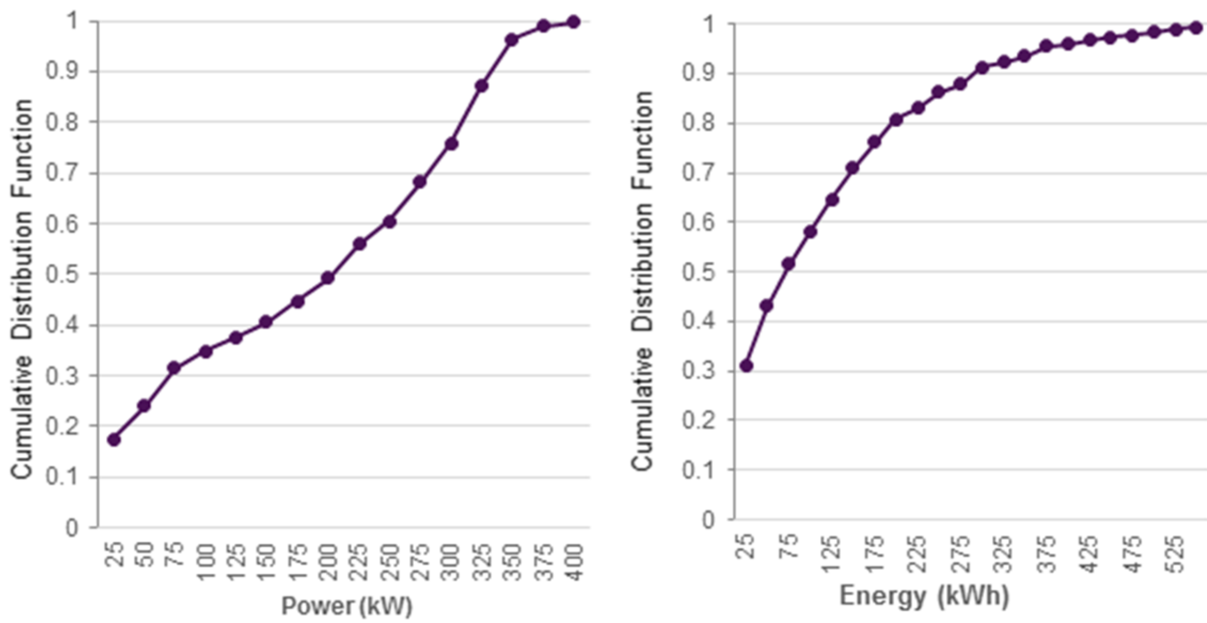

Figure 34. Commercial PV site cumulative distribution of error in power and energy.

The cumulative distribution of the error functions for power and energy are given in Figure 34. Based on these distribution functions, an ESS at the commercial PV site rated at 300 kW and 200 kWh (40 minutes of storage) will successfully compensate for power and energy differences compared to forecast values in 80% of the cases and partially compensate for the remaining 20%. An ESS of 475 kW and 275 kWh (35 minutes of storage) at Doney Park PV plant will completely compensate for power and energy differences in 80% of cases and partially compensate for the remaining 20%.

The measured PV output power at the commercial PV site for a cloudy day (Figure 35) is chosen to simulate the effect of the ESS. With proper controls, the output power errors are reduced from 350 kW to 50 kW and the energy errors are reduced from 249 kWh to 49 kWh.

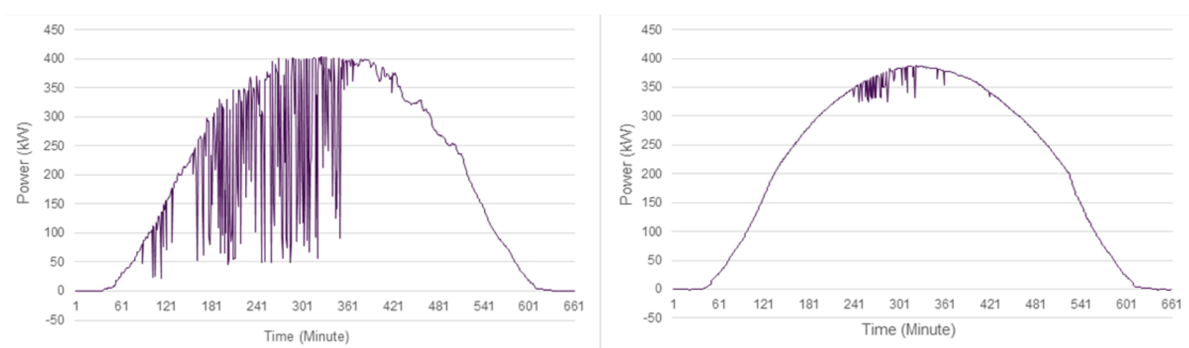

Figure 35. PV plant output at Cromer on Jan 11, 2013, without and with ESS.

Smart inverters are then used to smooth the voltage variations (Figure 33) due to cloud cover and high penetration. To verify the capability of the smart inverter to smooth out fast voltage sags due to cloud transients, the worst case power drop from rated power to zero in one minute is considered. The reactive power capability of the inverter increases when the output power drops. The power ramp rate and reactive power injected by the inverter at the commercial PV site are shown in Figure 36. The voltage sag caused by this power ramp is shown in Figure 37. As shown, the smart inverter has enough capacity to completely smooth the voltage sag due to worst case power ramp rate.

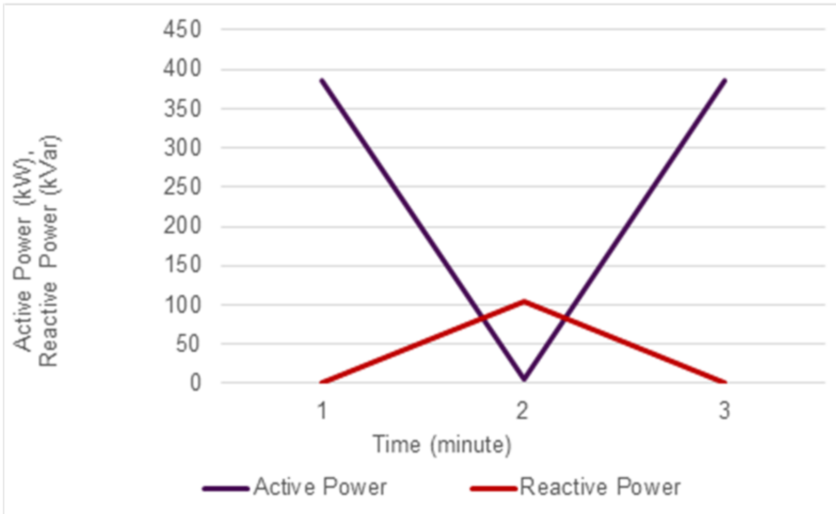

Figure 36. Power ramp and reactive power capacity of smart inverter at commercial PV site .

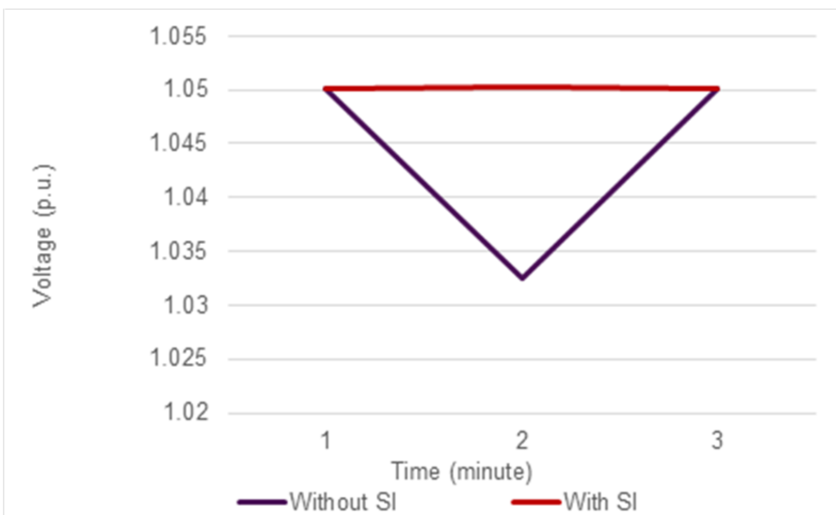

Figure 37. Voltage profile at commercial PV site bus due to worst case power ramp.

Based on this analysis, one can conclude that:

- Energy storage can be sized to mitigate most of the real power variations due to cloud cover.
- During peak power production, the smart inverter cannot completely mitigate voltage violations, but it can reduce the duration of the violation.

- Smart inverters can smooth the fast voltage variations due to cloud cover by providing reactive power.

7. Cost Benefit Analysis

From the inception of the project, multiple strategies were being considered as potential solutions to a PV hosting constraint, the team envisioned a method was needed to compare the relative merits of each strategy. During the requirements gathering phase of the task, the team defined the following considerations as being important to the construction, implementation and usability of the intended solution.

1. Adherence to common utility practice for costing distribution projects
2. Ability to report usable information with varying levels of input detail (low to high)
3. Easy accommodation of new mitigation options
4. Scalability & transportability (ability to be migrated to other platforms)
5. Ability for rapid prototyping and development given tight schedule

Microsoft Access® 2010 was chosen as the platform for the tool as it successfully addresses many of these requirements. The team reviewed costing spreadsheets, in use by the utility's distribution planning department, to develop the structure for the cost benefit and alternatives analysis, and to determine an appropriate metric for ranking identified alternatives for reducing the impact of new intermittent renewable energy generation source. After much debate, the team agreed to use net present value for that ranking.

The intended work flow as described in the interconnection flow chart Figure 6 is once constraints are identified—such as a voltage violation due to an existing or new forecasted PV plant—an engineer or analyst would perform advanced scenario analysis to determine strategy configurations to mitigate the project's impact. The required equipment configuration and the energy profile of the baseline and alternatives, then become inputs to the cost benefit tool.

The other major inputs to the tool are:

- Company-wide financial parameters (envisioned to be pre-populated and updated semi-annually)
- Work package setup (describing the various equipment/O&M needed for each mitigation strategy, including equipment and labor costs)

The tool is currently configured to calculate net present value based on these parameters and to display a high level summary for the user, with the alternatives sorted based on 10-year NPV. The detail information is able to be exported directly to Microsoft Excel® or other tool for further analysis or presentation. The team expects further refinement and evolution as the host utility gains fluency with the tool and its analysis capabilities (including, perhaps, alternate economic figures, custom output, etc.).

8. Conclusions and Recommendations

Phase 1 provided many insights into the process behind implementing high penetration PV projects. Some of the major conclusions from Phase 1 are as follows:

Careful consideration must be given to designing a data acquisition system for use in high penetration PV cases. The system must be designed to capture and synchronize both electrical and environmental data with sufficient resolution to adequately capture a variety of potentially disruptive phenomenon. Transmitting and synchronizing these data even on a small scale can provide significant storage and communication challenges.

Accurately modeling distribution feeders to the level necessary to analyze the impacts of high penetrations of intermittent resources is an involved process. Even though a utility may have data from various separate databases (GIS, DMS, etc.) describing their systems in significant detail, (since these databases were not intended to be used for model development), gaps and inaccuracies may manifest in electrical models developed from these sources. Even with detailed analysis, building a model that accurately represents the electrical system down to the customer meter will likely be an iterative process, checked and re-checked against data from field devices.

Utilities have gathered great experience in the application of rotating power generation equipment, and some also have experience with power electronic aided energy shaping. However, many utilities are just beginning to add large and small scale power electronics to their grid. Power electronic systems, such as the PV inverter described in this report, offer many potential benefits to utilities but behave differently than traditional generation. Lack of familiarity with this new technology and lack of results from field demonstrations can lead to hesitation on behalf of the utility in going forward with broader power electronic based solutions. A major goal of this project was to demonstrate these capabilities in order to assist APS (and other interested utilities) in gaining experience and familiarity with power electronics, their requirements, and their potential economic and operational benefits.

In order to achieve higher PV hosting capacity, future feeders will include distributed smart inverters – a few, large utility-scale inverters (MW level) whose output characteristics or settings can be remotely controlled by an utility operator, and numerous residential roof-top *grid-supportive* inverters. Future feeders will include strategically placed energy storage, load tap changing transformers at the substation that operate based on the load and solar insolation conditions, and high bandwidth measurements (at a minimum voltage measurements) to provide operational information for the control systems in advanced PV inverters, energy storage, LTC, and other data aggregation and control nodes.

8.1. Load Tap Changing Transformers at Substations

A key challenge in achieving higher hosting capacity as described in earlier sections is the potential feeder voltage violation. Cost effective mitigation of the voltage violation issue will involve the optimal design and coordinated use of each of the above techniques – smart inverters, energy storage and Load Tap Changer (LTC). Significant increase in hosting capacity can be obtained even without storage and smart inverters by appropriate tap selection of LTC based on load and irradiance and/or voltages at selected nodes. As an example, with PV generation at 200% of the base hosting capacity, there are 800 buses that violate ANSI voltage limit over a day in SV04 when no mitigation measures are taken. This reduces to 145 buses if an LTC is used and the appropriate tap is used constantly. If the LTC is allowed to make two tap changes a day based simply on time-of-day, the number of violations reduces further to 91 and the magnitude of violation is also reduced. Hence, the requirement on energy storage or reactive power from a smart inverter can be significantly reduced with LTC.

8.2. Reactive Power Support from Residential PV Inverters

Another cost effective way to maintain feeder voltage profile within limits under high PV penetration levels is the use of reactive power capability of advanced inverters. The utility-scale inverters, which are few in number, can be designed to regulate their terminal voltage (or the voltage at a critical remote bus) by closed-loop control, with their settings and relevant parameters being controllable remotely by the utility operator. These inverters will have advanced features including volt/VAR control, volt/Watt control, frequency based curtailment, full range of power factor control (0 to 1 leading and lagging) and sufficient margin for reactive power even while injecting rated active power. Many of the capabilities of these central, smart inverters have been demonstrated in this project through the field operation of GE Brilliance 700 kVA inverter.

The residential scale string inverters currently operate only at unity power factor however, depending on the topology used, many of the string inverters are also capable of providing on-demand reactive power support and variable power factor operation. Based on the emerging products from inverter manufacturers, it can be expected that in the near future, the string inverters will feature the capability for autonomously injecting reactive power and/or operate at fixed power factor mode and provide frequency based energy curtailment, all on a pre-determined schedule without real-time communication. Although some pilot projects are underway to demonstrate advanced features in residential string inverters[13] to be on par with central inverters, it is expected that in the near-term, the capabilities of the string inverters as well as the infrastructure for communication between the numerous string inverters and utility control center will remain limited.

Unlike the utility-scale inverters it may not be cost effective to have a large reserve capacity to inject reactive power at rated kW generation. The design of string inverters with a focus on cost and conversion efficiency may also restrict a wide range of power factor – emerging products seem to support up to 0.9 lagging and leading power factor. In this study extensive analyses were carried out to determine the effectiveness of advanced inverters, including residential inverters, in mitigating the impact of high penetration especially in terms of maintaining the voltage profile within ANSI limits. Table 12 shows the maximum voltage at any bus (including secondaries) on SV04 for

[13] In late 2014, APS initiated a project to deploy advanced residential inverters. The project is intended to explore requirements for communications and coordinated control of the inverters and their effects through field demonstration.

different high penetration scenarios. It is seen that reactive power absorbed at a power factor of 0.9 by each of the inverters is able to maintain the feeder voltage profile within limits even with PV generation 50% above the base hosting capacity. The case with PV 100% above the base hosting capacity failed to converge in OpenDSS simulation, but since at 50% above the maximum voltage was only 1.0381 p.u., it is expected that 0.9 power factor operation by all the inverters can result in voltages within limits up to 100% above base case, which is the maximum PV generation considered in this study. A separate task related to energy storage sizing to limit voltage violation also concluded that with reactive power support corresponding to 0.9 power factor, no energy storage would be needed based solely on voltage limits.

Table 12. Maximum Voltage at Different PV Levels

Power Factor	PV at base hosting capacity	PV at 15% above base hosting capacity	PV at 25% above base hosting capacity	PV at 50% above base hosting capacity
0.99	1.0454	1.0467	1.0476	1.0526
0.98	1.0433	1.0444	1.0451	1.0472
0.95	1.0393	1.0396	1.0399	1.0406
0.9	1.0381	1.0381	1.0381	1.0381

Based on the results from SV04 it is recommended that the residential inverters (typically in the 2 kW to 8 kW range) have a kVA rating of at least 1.11 times the maximum kW rating of the corresponding PV arrays. This corresponds to a reactive power capacity of 48.4% of the rated active power even when injecting rated active power. The inverters should also have the capability to adjust the PV operating power factor from unity to 0.9 lagging and leading. The control settings for the reactive power injection and/or power factor will be fixed at the time of installation and the inverters then operate autonomously based on the settings and local measurements such as terminal voltage and frequency. The settings themselves will be determined based on the distribution system characteristics such as the stiffness ratio, X/R ratio, specific location along the feeder, and proximity to voltage control devices and larger PV plants, for which extensive feeder modeling as done in this study on SV04 will be required. The settings can also be changed as new devices, new PV systems and loads are added.

8.3. Protection Coordination

Detailed analysis on protection coordination under high penetration scenarios in SV04 revealed the potential for reduction in sensitivity or reach of reclosers and relays for remote faults, and in some instances possibility of loss of coordination. The study assumed a worst-case value of 2 p.u. continuous fault current contribution from PV inverters for the duration of the fault. As more information on the fault characteristics of PV inverters becomes available these assumptions may be refined.

A key recommendation related to protection coordination is that the feeder be modeled in full detail as was done in this study using the multiple automated model development and analysis tools developed in this study. The model should be verified for different scenarios of fault conditions with and without PV systems and for various levels of penetration. A key area of focus is the reduction in fault current seen by the substation relay and reclosers as the PV penetration increases. The reduced current may require change of pick-up current settings or may even require additional reclosers which may not be required under low PV scenarios. Additionally, in feeders that employ fuse saving strategy, the analysis under various PV penetration levels should be carried out for fuse-recloser coordination as the potential for nuisance fuse blowing increases with PV penetration levels. In the future, adaptive settings for the relays and reclosers that change with measured operating conditions (irradiance levels and load) may be considered.

In the scenarios considered in the study, which extend up to penetration levels of around 100%, there were no instances of a recloser or relay tripping for faults upstream of these devices due to reverse current contribution from PV inverters. Even though reverse currents through the recloser were observed in simulation and measurement, they were not high enough to cause tripping of the reclosers for an upstream fault. Hence, the need for directional relays does not arise for the cases studied with the radial SV04 feeder. When feeder reconfiguration and networked distribution systems are considered however, protection devices with directional capability may be required.

8.4. Energy storage

The optimization tools developed in this study can be used to design the kW and kWh ratings of energy storage needed for different levels of PV and for different objectives to be met. The tools can also be used to obtain optimal scheduling of the storage.

An energy storage system is an effective mechanism for load shifting and peak shaving hence in enhancing the value of PV systems. In some cases ESS also allows deferral of upgrading distribution system equipment under high PV penetration scenarios. Some states are starting to include energy storage provisions in their renewable energy portfolio requirements. However, based on this study on SV04 and at the penetration levels considered (maximum of around 100% penetration), the combination of smart inverter control with sufficient margin for reactive power injection at full power and a load tap changing transformer can mitigate the impact on the feeder voltage profile without large scale energy storage. Based on the study it can be concluded that if energy storage is designed for load shifting and peak shaving purposes and for deferral of upgrading distribution equipment like transformers and line conductors, then the same ESS can also be used as one of the mitigation tools to support high PV penetration. The control of ESS will then be integrated into the overall distribution system control and operation.

8.5. Need for Inverter Models

A main limitation in the modeling process and analysis is the lack of sufficient details on the design and characteristics of the utility-scale and residential inverters. Specifically, the algorithms and parameters used in island detection schemes employed in the inverter are needed for an accurate study of the impact of high penetration with different inverter designs on the safety aspects related to unintentional islanding. The details on the output stage filter configuration and inductance and capacitance values, information on the switching frequency and type of pulse-width modulation (PWM) used (unipolar, bipolar, hybrid PWM) are also very important for accurate analysis on high penetration impact in terms of high frequency content in the feeder voltage and power quality. As the inverters move toward more advanced features such as volt/VAR control, and as the penetration levels increase with inverters of multiple designs operating in close proximity, it will be important to obtain the specific control algorithms and parameters used in these system- level control loops, in order to determine potential for unstable interactions among multiple inverters. Distribution system analysis tools such as OpenDSS allow use of dynamic linked libraries (DLL). These DLLs may be a possible way for the manufactures to provide models which accurately capture the characteristics of interest to the distribution system designer without sharing much of the proprietary control design information which could be masked in the DLL model.

9. Budget and Schedule

The project schedule is shown in Table 13. There were five no-cost extensions granted to APS over the course of the award, a total of seventeen contract modifications, and no spend plan slips.

Table 13. Budget and Schedule

Budget Period	Start Date	End Date
Period 1/Phase 2	01/01/2011	10/31/2012
Period 2/Phase 3	07/01/2012	05/31/2013
Period 3/Phase 4	06/01/2013	04/30/2014
Period 4/Phase 5	05/01/2014	02/28/2014

The final approved budget is shown in Figure 38. This includes category totals, including the DOE and APS cost share amounts.

Recipient:	Arizona Public Service Company
DOE Award #:	DE-EE0004679

Spending Summary for SF 424A Budget Forms

Object Class Categories	APPROVED BUDGET	TOTAL SPENT TO DATE	Forecasted Spending (FINAL COSTING FOR FY15 SCOPE)
a. Personnel	$396,698	$348,867	$19,000.00
b. Fringe Benefits	$188,513	$158,510	$8,573
c. Travel	$19,275	$19,368	$0
d. Equipment	$0	$0	$0
e. Supplies	$34,622	$34,668	$0
f. Contractual	$2,676,027	$2,398,331	$300,090
g. Construction	$0	$0	$0
h. Other	$25	$25	$0
i. Total Direct Charges (sum of a to h)	$3,315,160	$2,959,769	$327,662
j. Indirect Charges	$41,779	$41,413	$2,012
k. Totals (sum of i and j)	**$3,356,939**	**$3,001,182**	**$329,674**
DOE Share	$2,727,943	$2,420,924	$253,908.55
Cost Share	$628,996	$580,258	$75,766
Calculated Cost Share Percentage	18.7%	19.3%	23.0%

Figure 38. SF 424A budget form summary.

10. Path Forward

In January 2015, APS initiated its Solar Partner residential rooftop solar program, which will generate up to 10 MW of electricity through 1,500 APS-owned residential rooftop solar systems. APS will operate and maintain the equipment while paying selected customers $30 per month through the life of the 20-year program. The project will include residential grid-support inverters and energy storage. APS will examine various use cases to gain critical knowledge in areas such as capacity control, voltage management, market driven dispersion and battery storage. All rooftop solar systems will incorporate advanced inverter technology and be strategically located in areas where specific electrical distribution feeders can be studied to learn how to better integrate solar onto the APS grid. APS will also orient each system in a west to southwest manner to obtain maximize afternoon capacity match. This project provides a platform for validating and extending the methods and tools developed during this study and APS intends to apply them to inform and monitor the deployment and to further study the potential issues associated with high penetration solar.

11. Bibliography

11.1. Presentations

R. Ayyanar, “Distribution System Analysis Tools for Studying High Penetration of PV with Grid Support Features,” PSERC public webinar, December 2013

B. Mather, R. Meeker, D. Narang, M. Rylander, “’Beyond PV “Percent Penetration (15%)’ ; Myth or Fact” presented at DistribuTECH 2014 Conference and Exhibition, San Antonio, TX, January 2014

D. Narang, L, Hannoush, Sunshot Grand Challenge Poster Presentation (May, 2014)

M. Baggu, “Advanced Inverter Analysis and Demonstration on a Distribution Feeder” presented at the 2014 PV Distribution System Modeling Workshop, Santa Clara, CA, May 2014

Y. Tang, R. Ayyanar, “Verification of protective device coordination in distribution systems with photovoltaic generation,” IEEE 40th Photovoltaic Specialist Conference (PVSC), 2014, pp. 2100-2105

A. Nagarajan, R. Ayyanar, “Application of Minimum Spanning Tree algorithm for network reduction of distribution systems,” North American Power Symposium (NAPS), 2014, pp. 1-5

A. Nagarajan, R. Ayyanar, “Modeling large distribution feeders for transient analysis using graph search algorithms,” North American Power Symposium (NAPS), 2014, pp. 1-5.

T. Yao, Y. Tang, R. Ayyanar, “High resolution output power estimation of large-scale distributed PV systems,” IEEE Energy Conversion Congress and Exposition (ECCE), 2014, pp. 4620-4627

Y. Tang, R. Ayyanar, “Modeling and validation of a distribution system with high PV penetration using zone division method,” IEEE PES T&D Conference and Exposition, 2014, pp. 1-5.

A. Nagarajan, R. Ayyanar, “Dynamic analysis of distribution systems with high penetration of PV generators using differential algebraic equations in OpenDSS,” North American Power Symposium (NAPS), 2014, pp. 1-6.

T. Joshi, G. Heydt, R. Ayyanar, “High frequency spectral components in distribution voltages and currents due to photovoltaic resources,” North American Power Symposium (NAPS), 2014, pp. 1-6.

A. Nagarajan, R. Ayyanar, “Dynamic phasor model of single-phase inverters for analysis and simulation of large power distribution systems,” IEEE International Symposium on Power Electronics for Distributed Generation Systems (PEDG), 2013, pp. 1-6.

P. Mitra, V. Vittal, G.T. Heydt, R. Ayyanar, “Effectiveness of anti-islanding schemes following a faulty recloser operation,” IEEE Power and Energy Society General Meeting (PES), 2013, pp. 1-5

P. Mitra, V. Vittal, G.T. Heydt, "The impact of distributed photovoltaic generation on residential distribution systems," North American Power Symposium (NAPS), 2012, pp. 1-6.

Y. Tang, X. Mao, R. Ayyanar, "Distribution system modeling using CYMDIST for study of high penetration of distributed solar photovoltaics," North American Power Symposium (NAPS), 2012, pp. 1-6.

D. Narang, P. Smithers, T. Tewelis, J. Wilhelm, "Optimizing Distributed Generation Through Smart Technologies", presented at DistribuTECH 2012 Conference and Exhibition, San Antonio, TX, January, 2012

11.2. Publications

P. Gotseff, J. Cale, M. Baggu, D. Narang, and K. Carroll, "Accurate Power Prediction of Spatially Distributed PV Systems using Localized Irradiance Measurements," *Power and Energy Society (PES) 2014*, submitted Dec 6, 2013.

M. Baggu, J. Cale, and D. Narang, "High-Penetration PV Deployment in the Arizona Public Service System, Results from Phases 3-4 and Update on (Final) Phase 5", *Photovoltaic Specialty Conference (PVSC) 2014*, draft to be submitted Jan, 2014.

M. Baggu, B. Palmintier, J. Cale, and D. Narang, "Distribution Modeling of Closed-loop Controls for Advanced Scenario Analysis on Feeders with High-Penetration PV", *Photovoltaic Specialty Conference (PVSC) 2014*, draft to be submitted Feb, 2014.

J. Cale, B. Palmintier, D. Narang, and K. Carroll, "Clustering of Distribution Feeders on the Arizona Public Service System", *Photovoltaic Specialty Conference (PVSC) 2014*, draft to be submitted Jan, 2014.

M. Baggu, R. Ayyanar, and D. Narang, "Feeder Model Validation and Simulation for High-Penetration Photovoltaic Deployment in the Arizona Public Service System", *Photovoltaic Specialty Conference (PVSC) 2014*, submitted May, 2014.

Y. Tang and R. Ayyanar, "Verification of Protective Device Coordination in Distribution Systems with Photovoltaic Generation", *Photovoltaic Specialty Conference (PVSC) 2014*, submitted May, 2014.

A. Nagarajan, R. Ayyanar, "Design and Strategy for the Deployment of Energy Storage Systems in a Distribution Feeder with Penetration of Renewable Resources," IEEE Transactions on Sustainable Energy, 2014, Article#: 2330294, IEEE Early Access.

T. Joshi, G. Heydt, R. Ayyanar, "High frequency spectral components in distribution voltages and currents due to photovoltaic resources," North American Power Symposium (NAPS), 2014, pp. 1-6.

Narang, David, Joshua Hambrick, Devarajan Srinivasan, Raja Ayyannar, Kathleen O'Brien, Jovan Bebic, and Owen Schelenz. 2011. "Final Technical Report: Results of Phase 1." doi:10.2172/1036532.
http://www.osti.gov/scitech/servlets/purl/1036532